Quantum Hall Array Structures Apply Quantized Resistance in the Wider World

Randolph Elmquist, Physicist, NIST, Gaithersburg, MD
Quantum Measurement Division

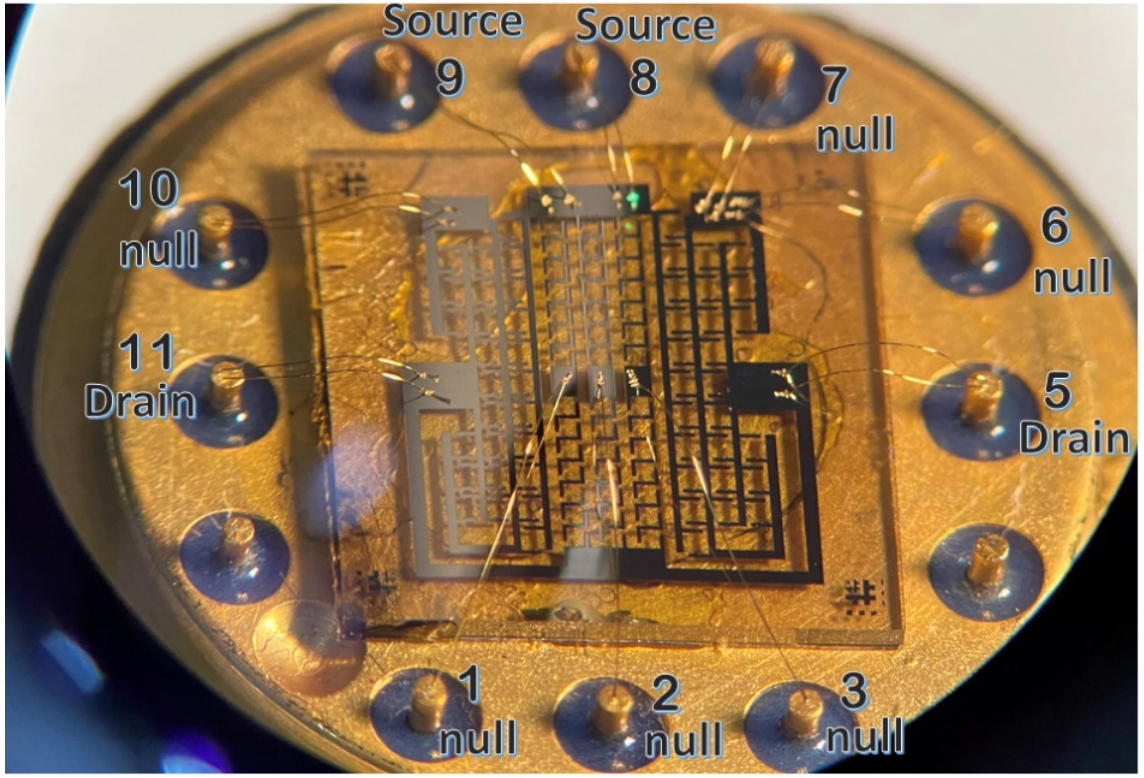

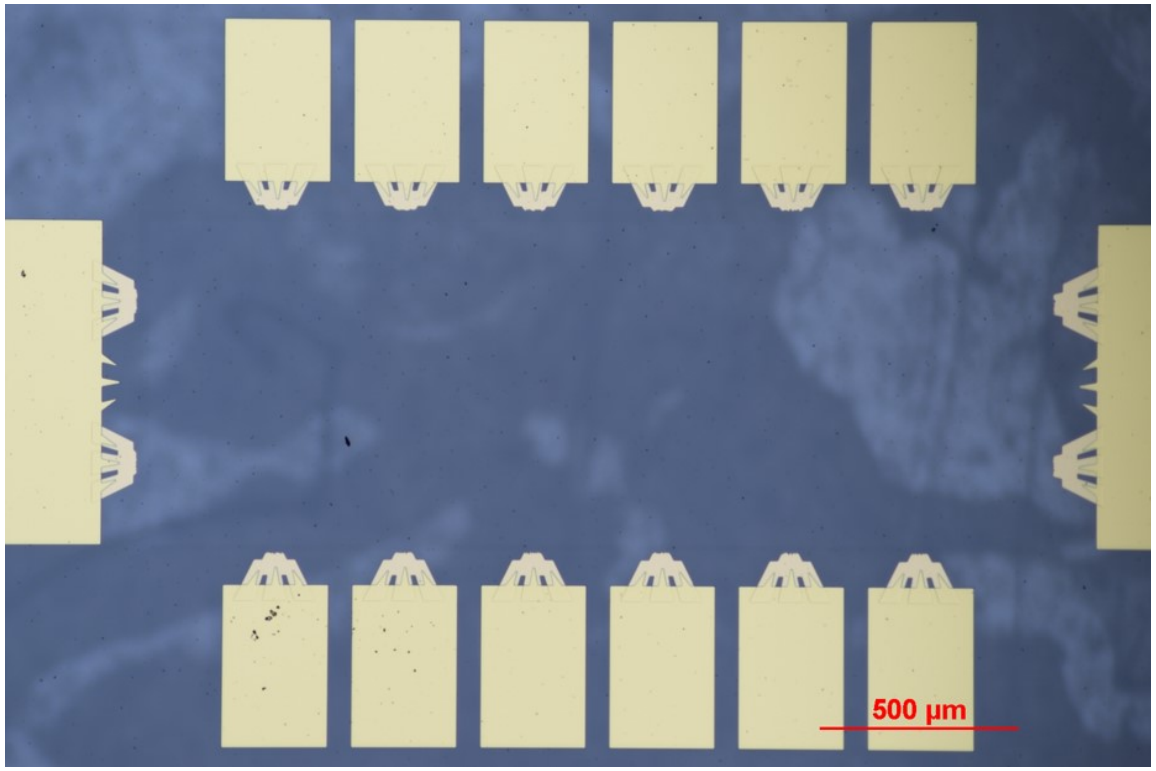

The International System (SI) is based on seven defining constants. Five of these defining constants are fundamental constants of nature. As such they are stable in time and space. But also, these constants are woven into the fabric of the universe, and they can, in principle, be accessed by every human. They are not owned, and they do not have to be locked away in a safe.

The seven defining constants are:

- the caesium hyperfine frequency $\Delta\nu_{Cs}$
- the speed of light in vacuum c
- the Planck constant h
- the elementary charge e
- the Boltzmann constant k
- the Avogadro constant N_A, and
- the luminous efficacy of a defined visible radiation K_{cd}

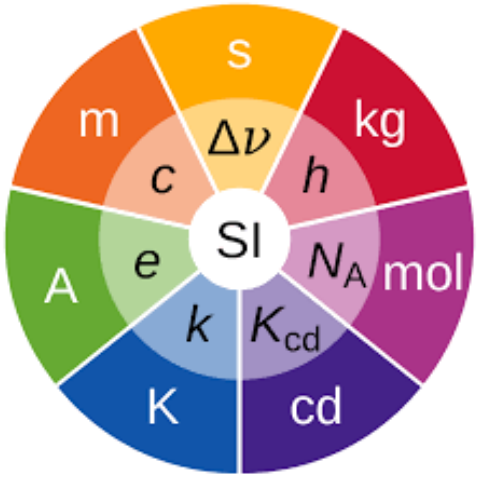

The numerical values of the seven defining constants have no uncertainty.

https://www.bipm.org/en/measurement-units/si-defining-constants

Quantum Hall effect in Graphene

$R_H = R_K/2 = 12906.4037217(42)$

U = 3.25 parts in 10^{10}

Source: From 2018 CODATA recommended values, the von Klitzing constant R_K = 25 812.807 45 . . . Ω

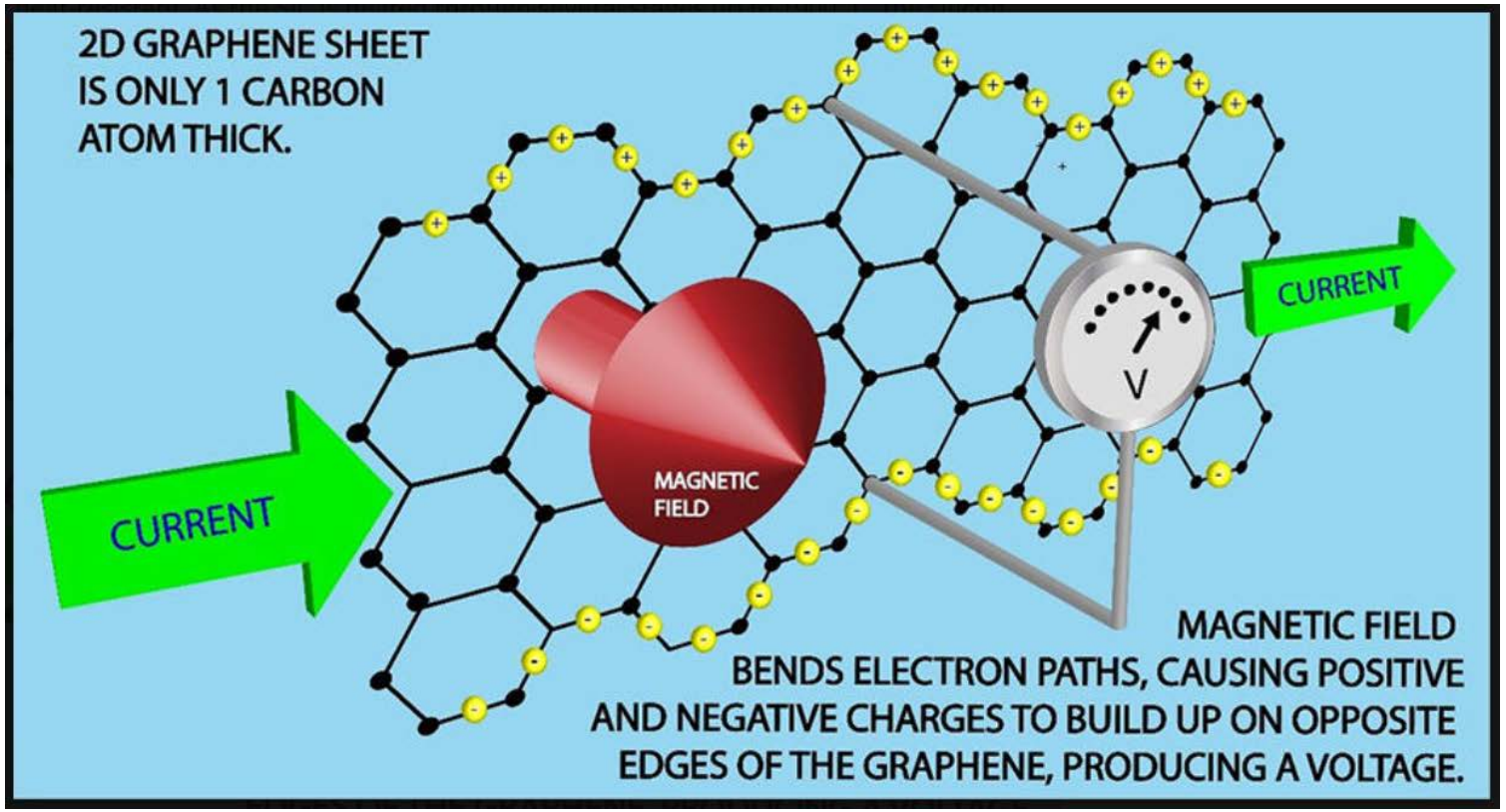

3D: **Hall effect voltage**

$V_H = IB/qnd$

I - current flowing in the sensor
B - magnetic field strength
q - charge
n - number of charge carriers per unit volume
d - thickness of the sensor

2D: **Quantum Hall effect**

$V_H = Ih/iq^2$

$R_H = h/iq^2$

h - Planck constant
q - charge
i - a quantum number given by number of states per unit area in a filled Landau level

Monolayer graphene devices, i = 2

Fabrication of Epitaxial **Graphene**:

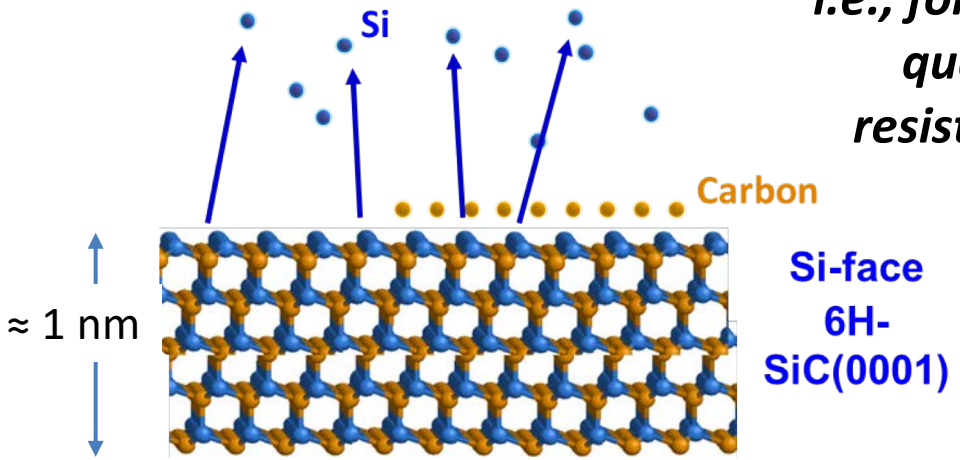

i.e., for monolayer quantized Hall resistance (QHR) standards

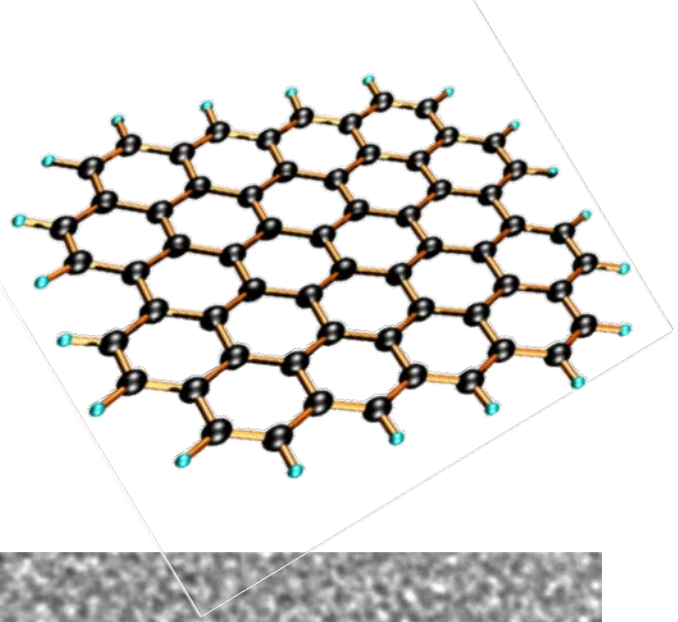

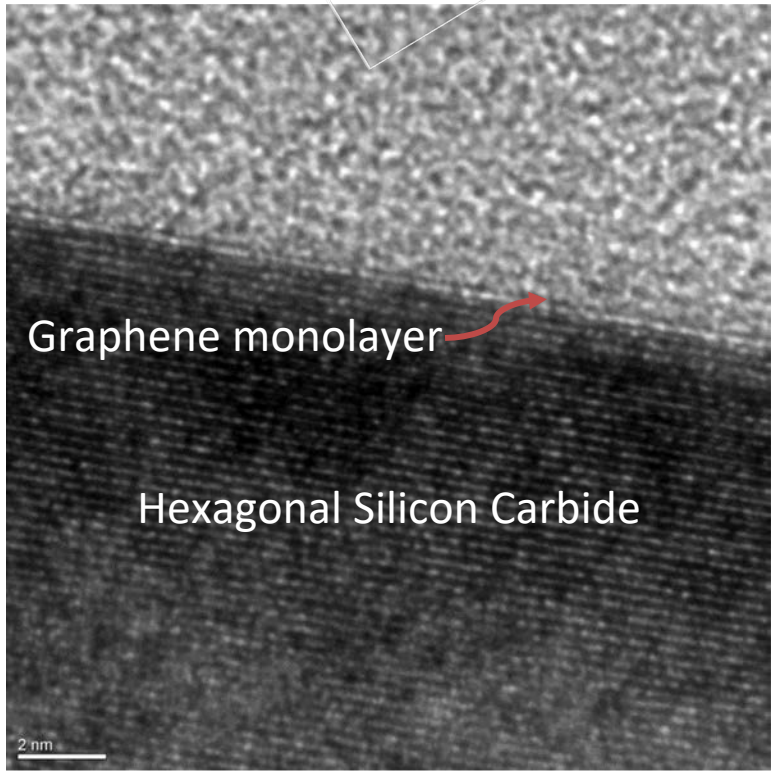

What's the measurement interest in all this?

Graphene is a two-dimensional (2D) conductor of electricity, similar to (but much simpler than) a GaAs heterojunction, as used for the quantized Hall resistance (QHR) standard:

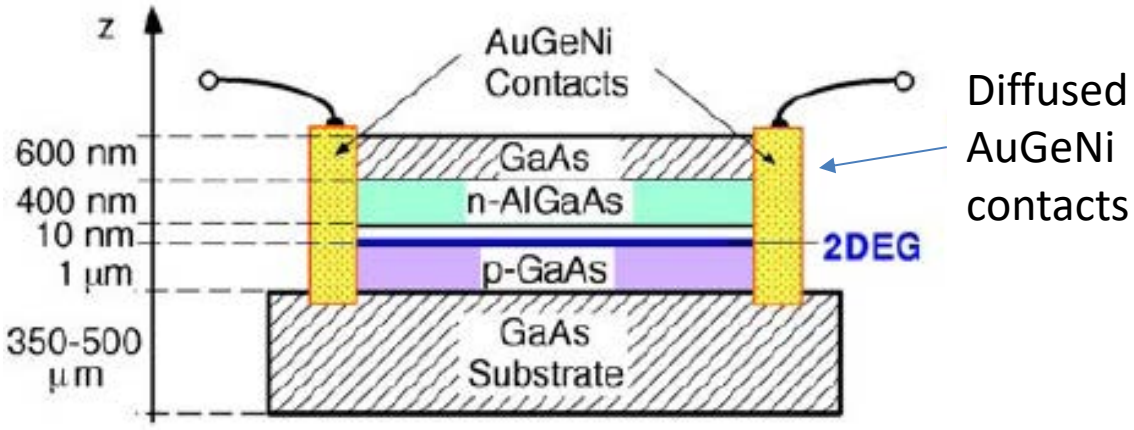

Diffused AuGeNi contacts

GaAs 2D conducting layers are created by semiconductor structures and are roughly 10 nm thick.

Sources:
MBE – Molecular beam epitaxy
MOCVD – Metal oxide chemical vapor deposition

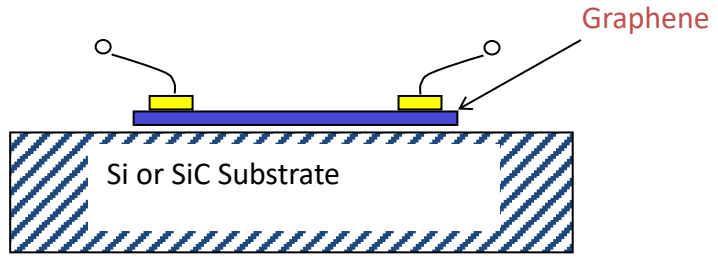

Graphene is a one-atom-thick carbon layer that freely conducts electricity in two dimensions.

Sources:
Exfoliated natural or man-made graphite
CVD – Chemical vapor deposition
SiC – Silicon Carbide epitaxial growth

Graphene flavors

- Exfoliated monolayers - electrical properties such as high mobility and an anomalous quantum Hall effect (QHE)

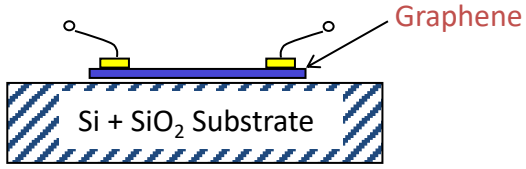

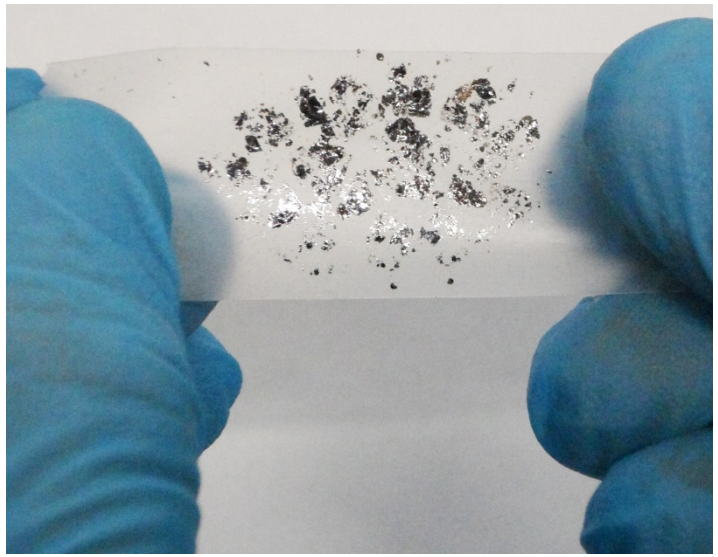

Control of layer number difficult

Size of devices is about 10 μm

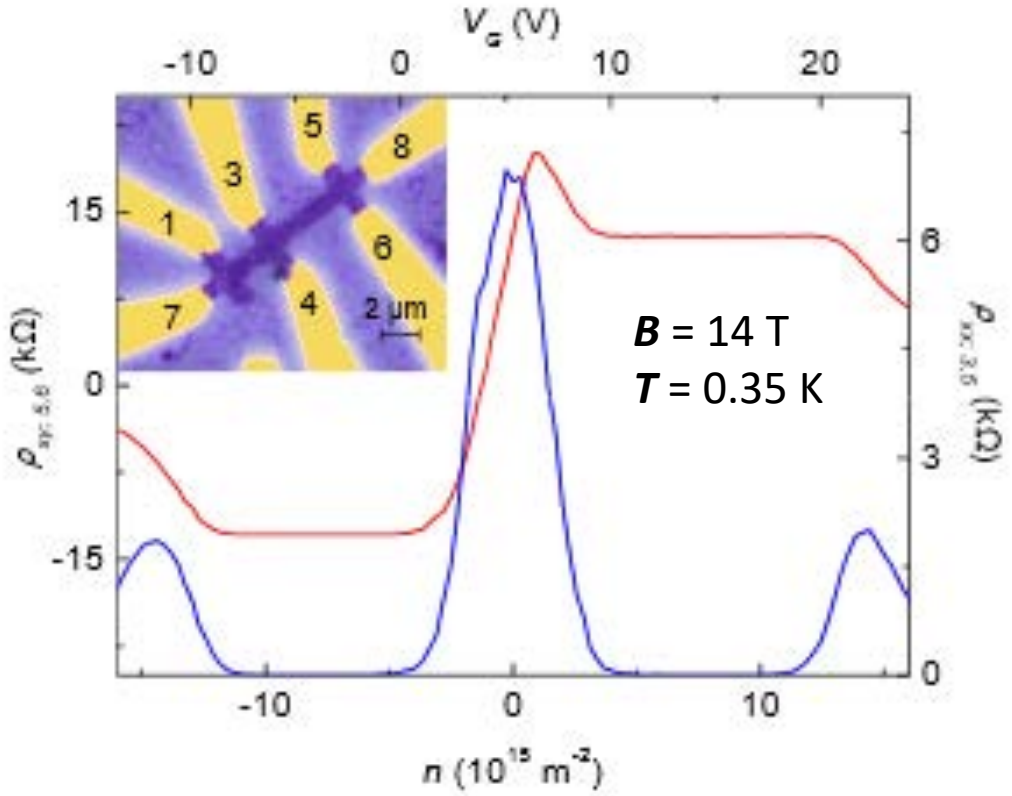

A. Geim and K. Novoselov, University of Manchester, UK

Graphene flavors - 2

- Chemical Vapor Deposition on Cu(111)

  - Growth stops at 1 layer
  - Domain size limited to that of substrate Cu domains
  - 200 μm – 2 mm domains

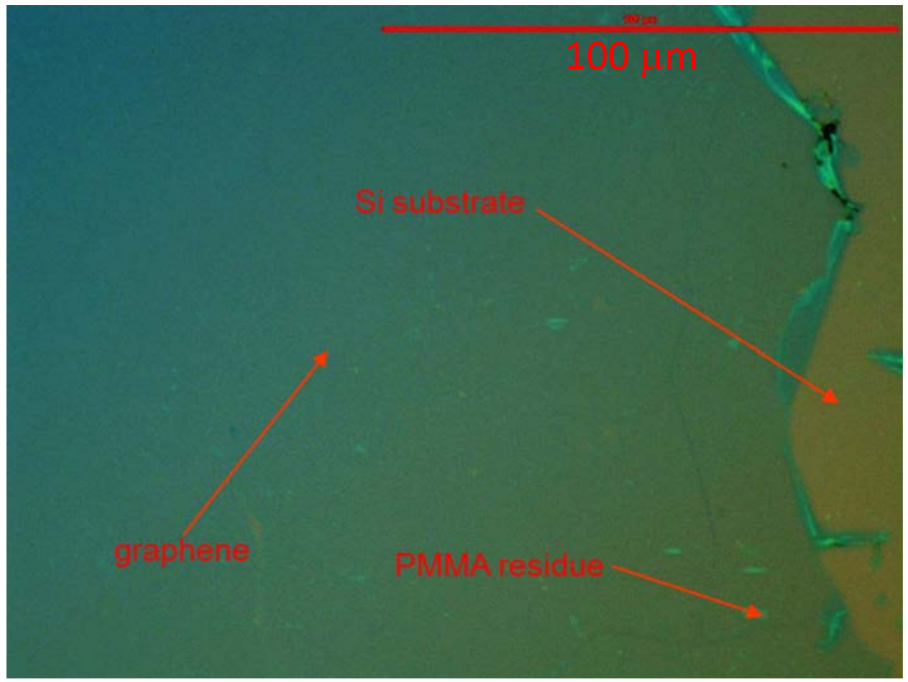

NIST, M. Keller and F.-H. Liu, 2013

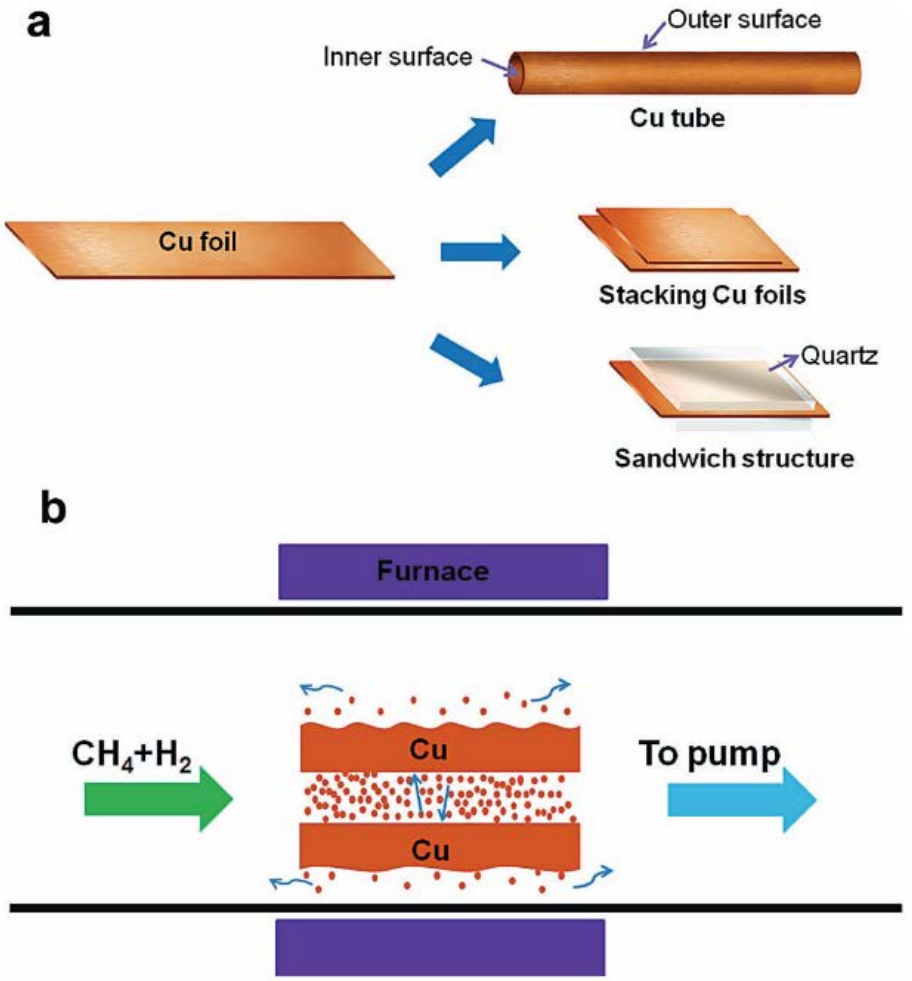

Figure 1. a) Cu tube, stacked Cu foils, and Cu foil between two quartz slides, prior to graphene growth. b) Illustration depicting the suppression of loss of Cu by evaporation and redeposition in a confined space during low pressure CVD growth of graphene.

S. Chen, *et al*., Adv. Mater., 25, 2062 (2013)

NIST Face-to-Graphite synthesis

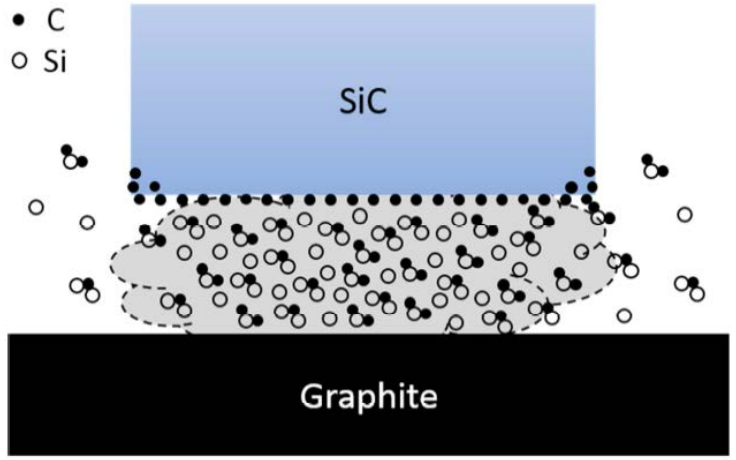

Ar (1900 °C)

Small **11**, 90-95 (2015)
Carbon **115**, 229-236 (2017)
Y. Yang, *et al*.

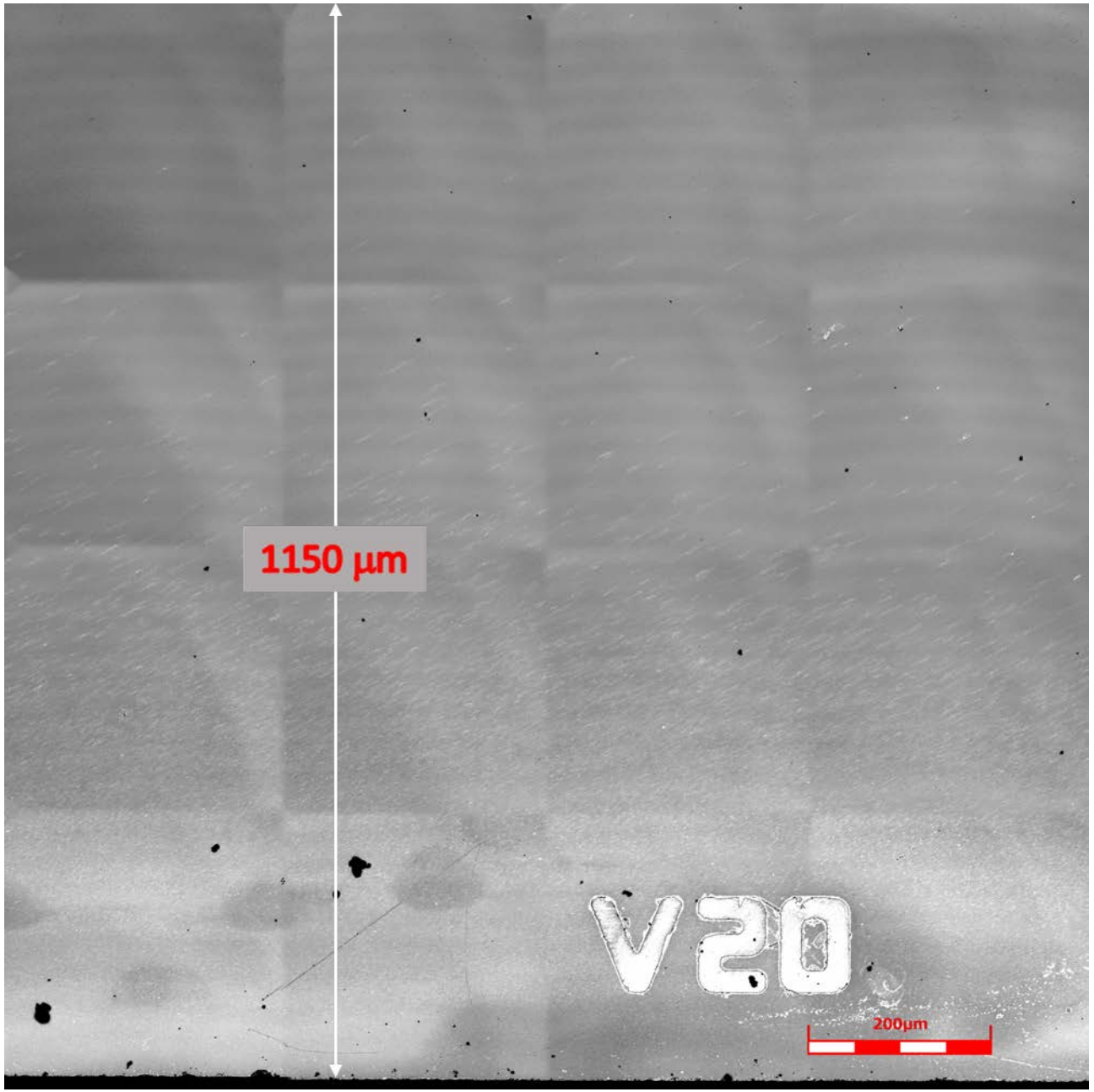

Gauging EG layer number

Nanostructure of graphene monolayer on SiC(0001) atomic terraces

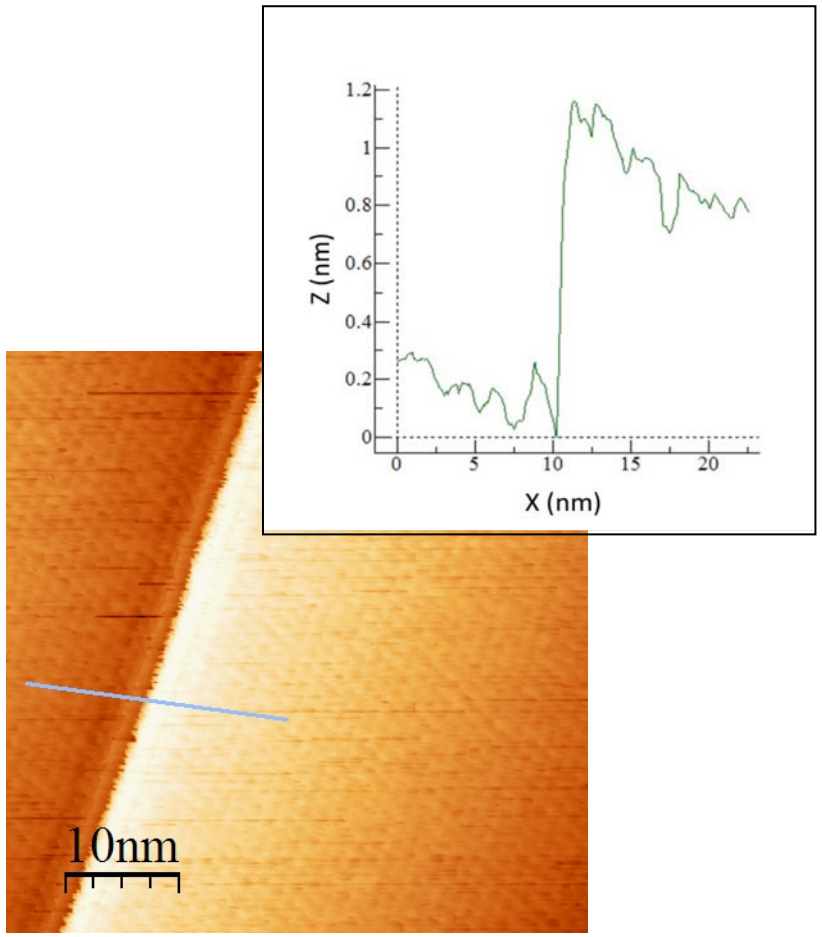

STM Topography (unfiltered)

Low-energy Electron Microscopy

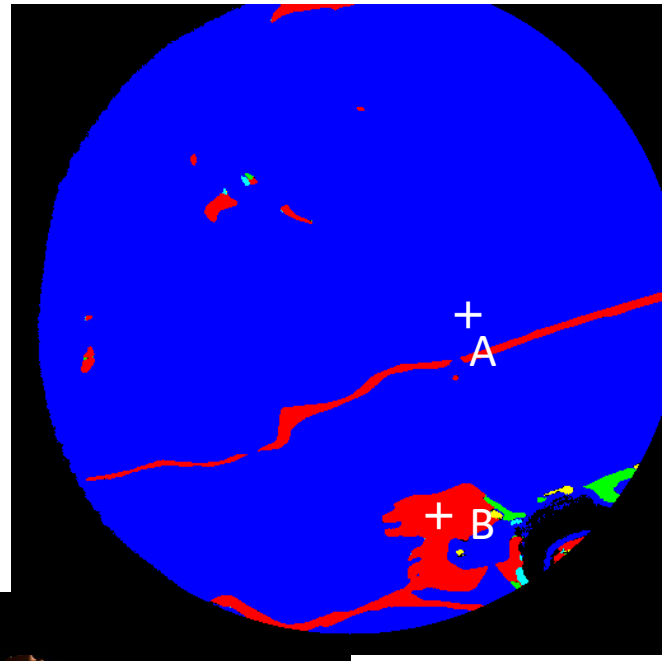

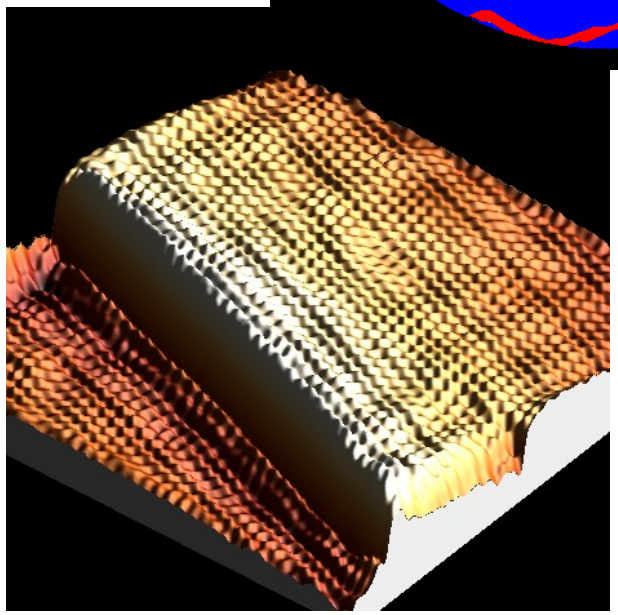

Above Image: Prof. R. Feenstra, Carnegie Mellon U. (diameter ~30 μm)

Lower images and data G. Shaw & J. Melcher, NIST

Epitaxial graphene monolayers

With face-to-graphite method, uniform monolayer growth is best achieved with minimum terrace size and low miscut.

2 hours 1200 °C (4% H_2 + Ar);
3 - 5 minutes at T =1900 °C

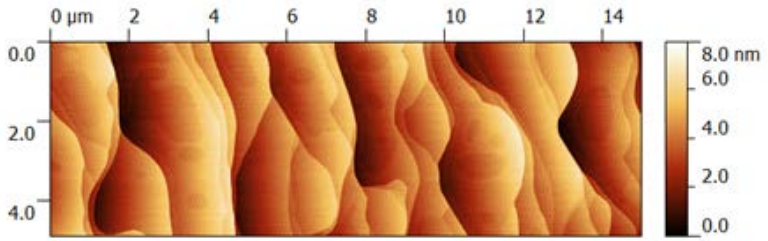

*Y. Yang, *et al*., *Small* **11**, 90-95 (2015)

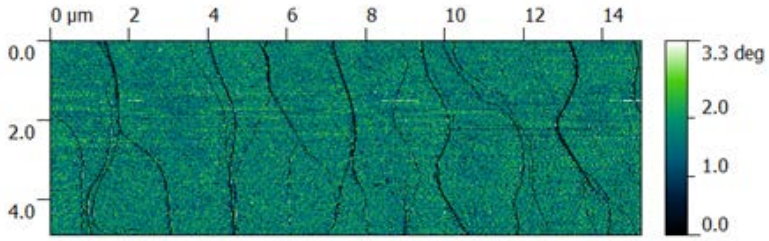

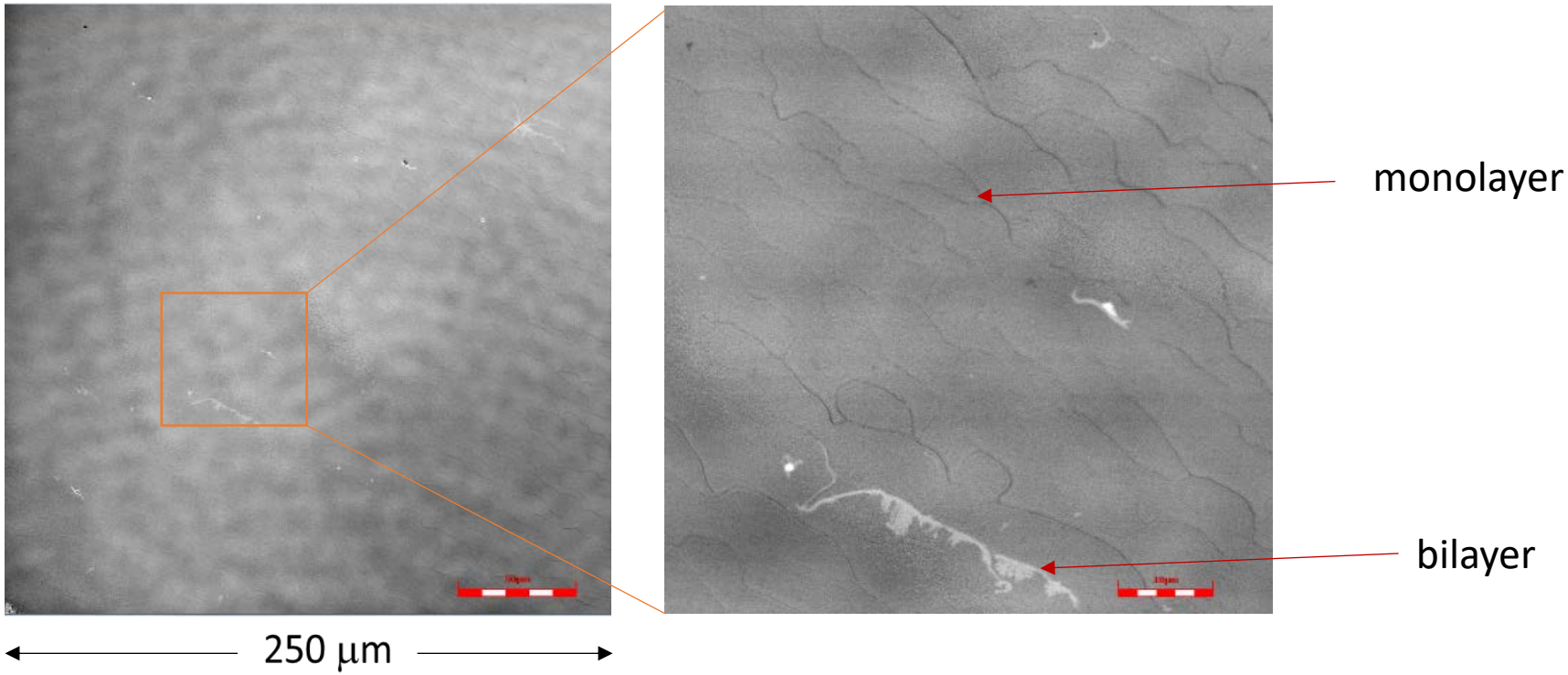

Face-To-Graphite EG synthesis

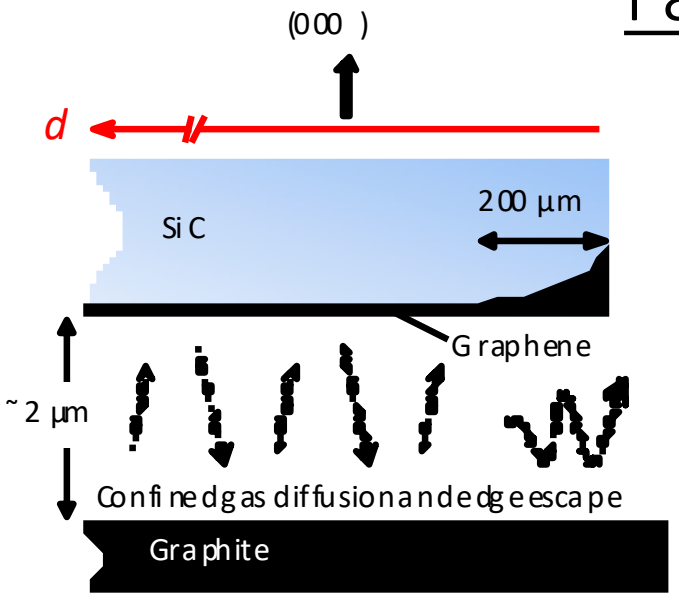

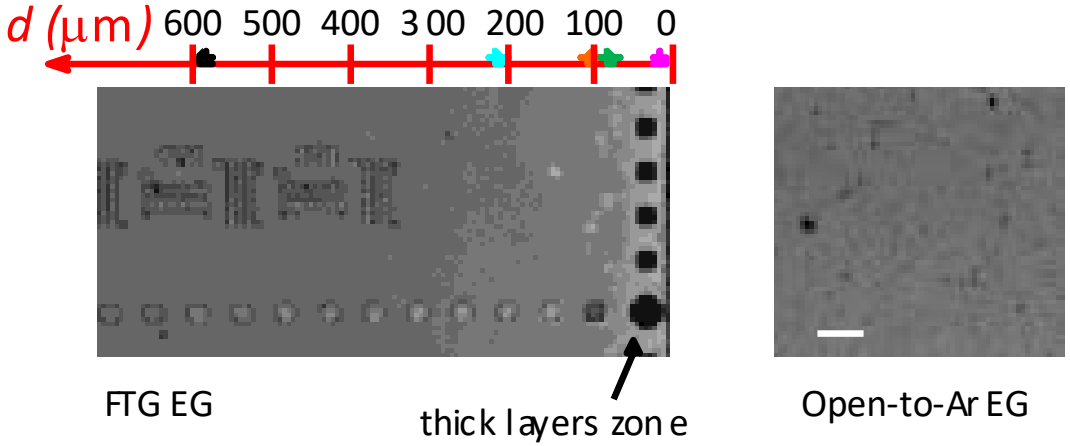

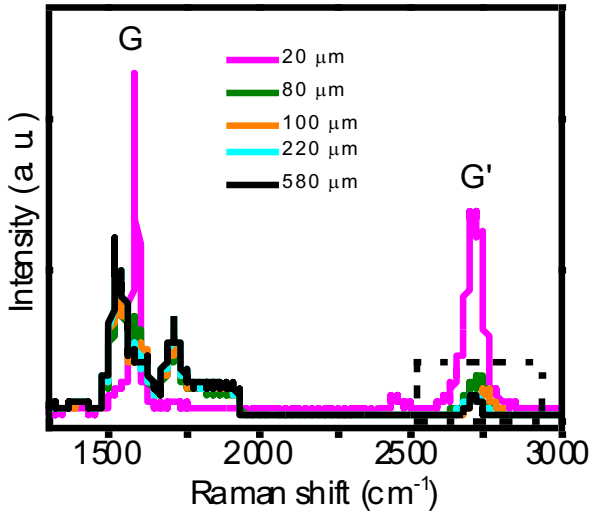

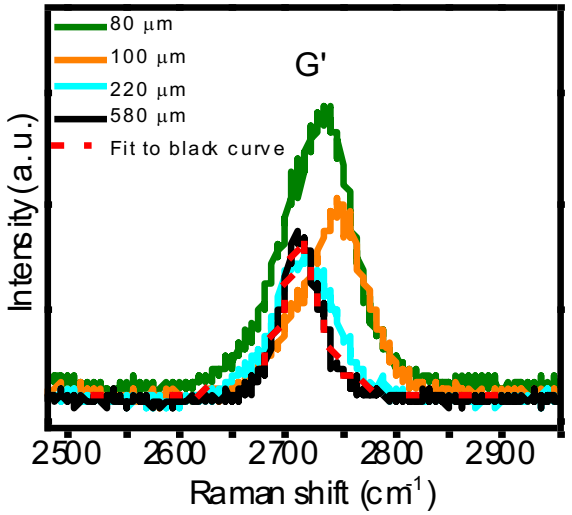

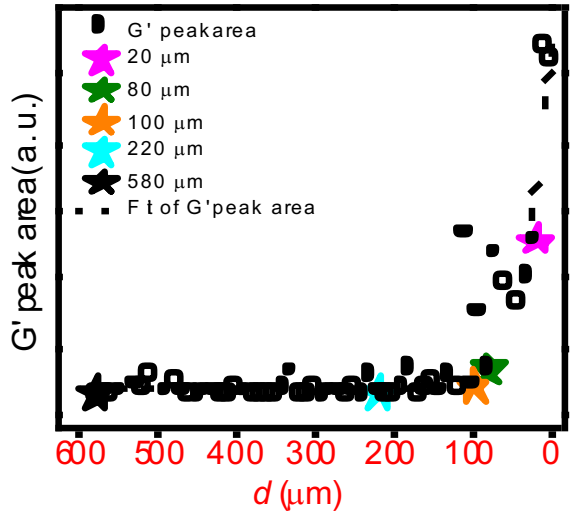

Yanfei Yang *et. al., Carbon* **115**, 229-236 (2017)

Graphene Quantum Hall for resistance standards

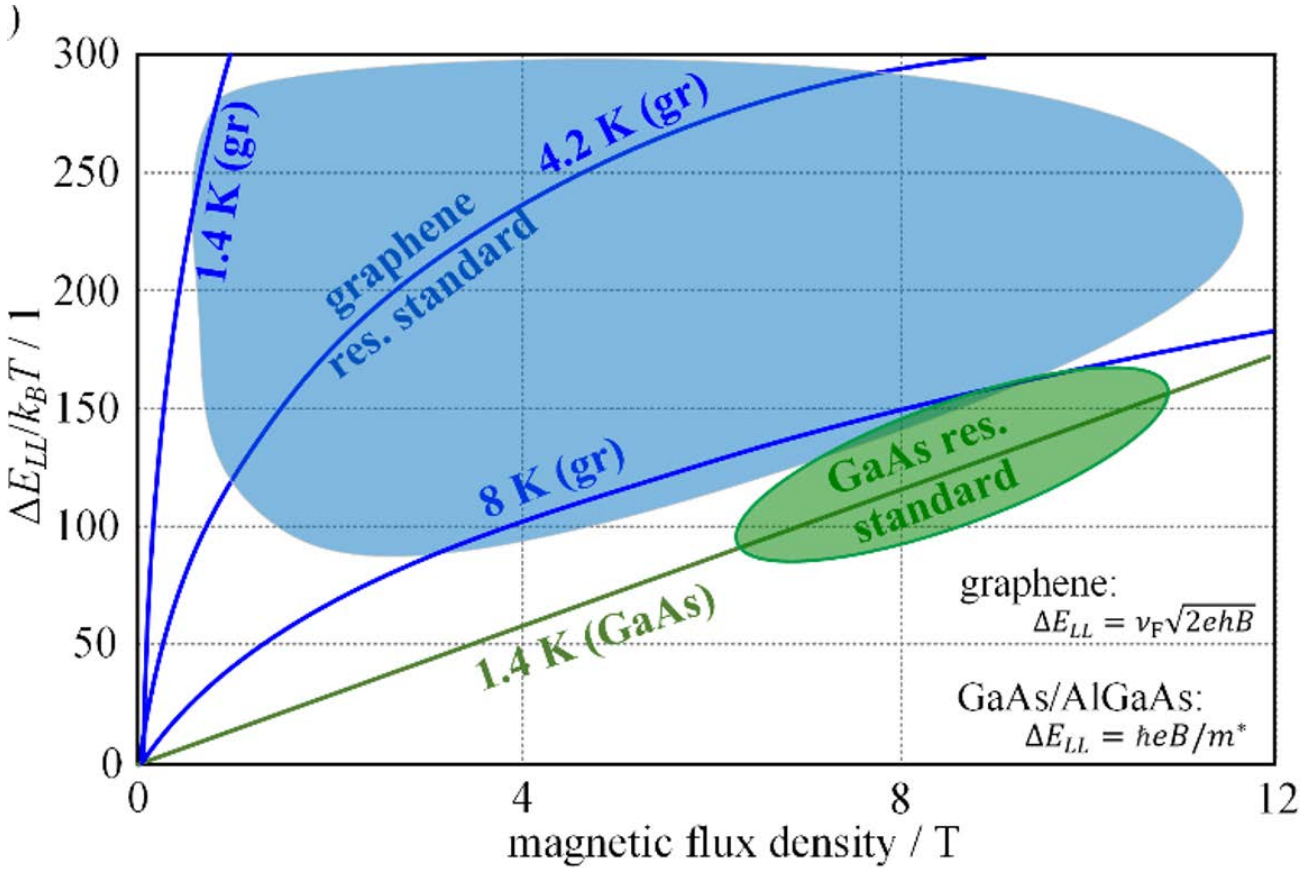

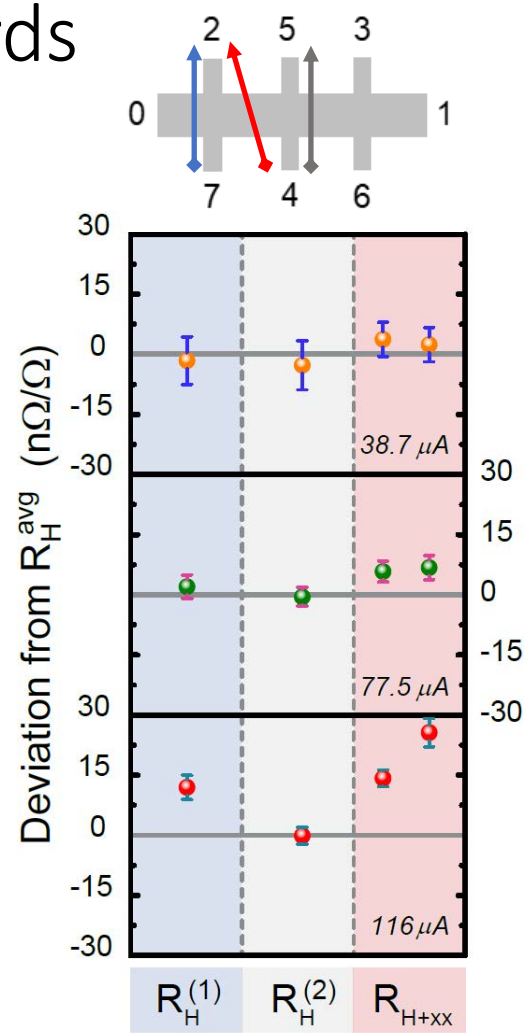

"Epitaxial graphene for quantum resistance metrology,"
M. Kruskopf and R.E. Elmquist, Metrologia 55 (2018) R27–R36

Graphene Devices for Table-Top and High Current Quantized Hall Resistance Standards, Rigosi et al., IEEE Trans. Inst. Meas. (2019)

- P-type graphene
- N-type graphene

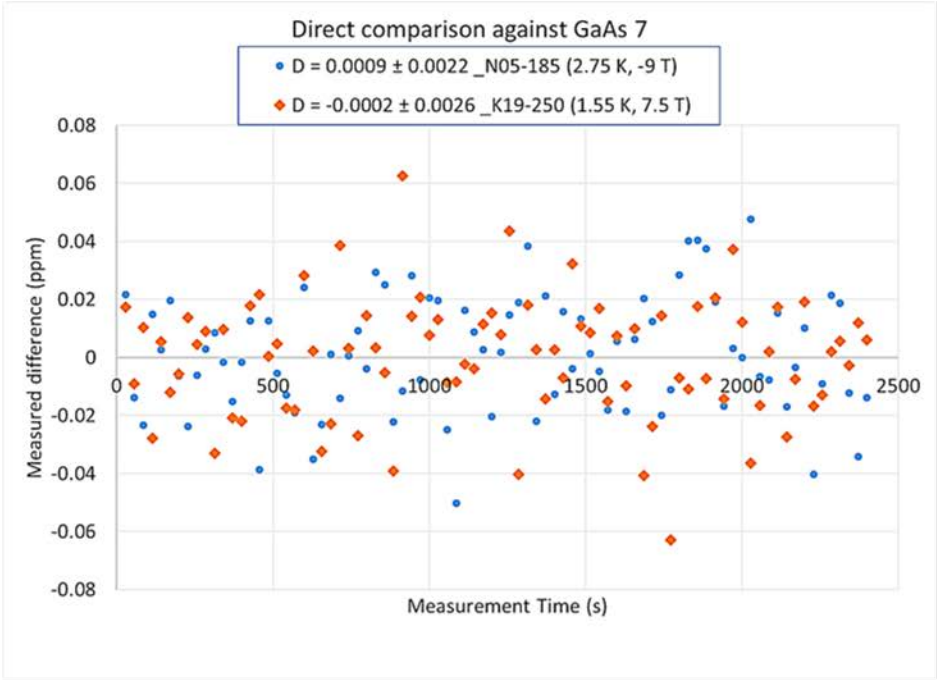

NIST QHR Standards

Quantum-Hall-bar can be located with relative precision onto high quality graphene

Hall bar design

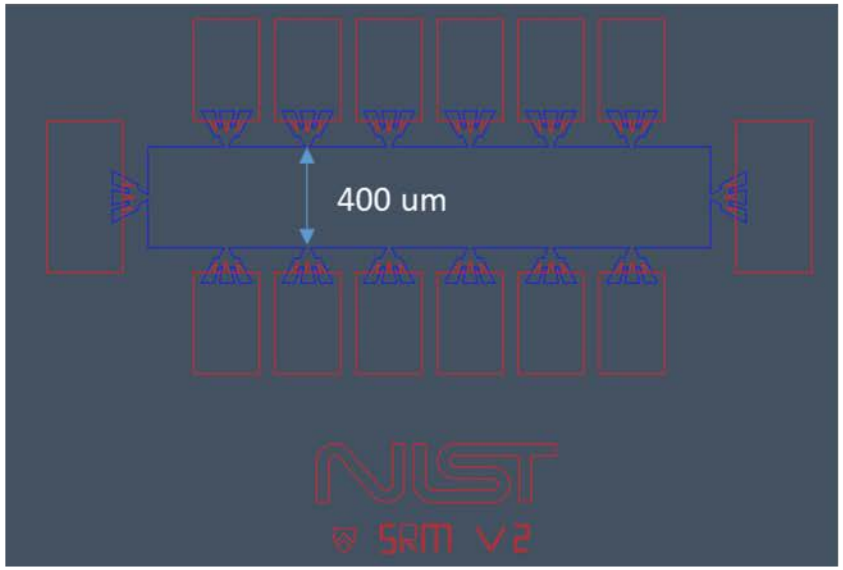

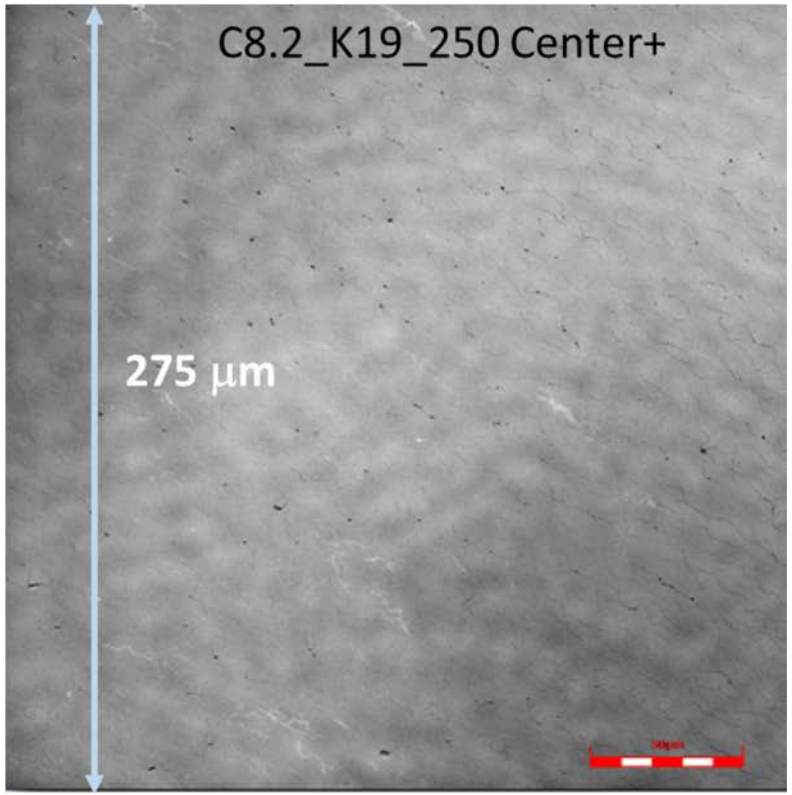

$CR(CO)_3$ complexes with rings of carbon atoms, with minimal distortion of the lattice

Induces strong p-type doping of graphene that counteracts n-type doping by the substrate

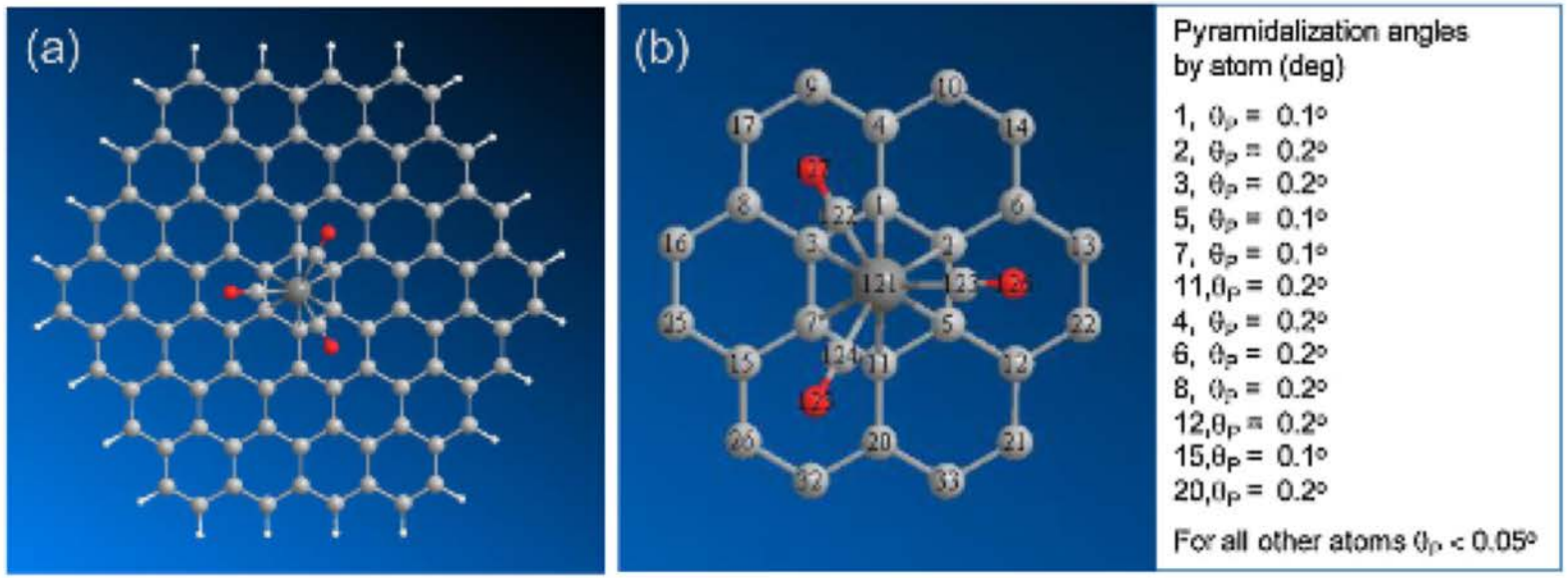

Fig. 8. Chem-3D structures of a $Cr(CO)_3$ unit complexed with a $C_{96}H_{24}$ graphene fragment obtained from the coordinates given by Gloriozov and coworkers (structure 4-Cr $(CO)_3$ in their notation) [58]. (a) Chem-3D structure of the complete $C_{96}H_{24}$-$Cr(CO)_3$ graphene fragment, (b) Sub-Unit, with numbering and calculated POAV pyramidalization angles (θ_p, deg).

Molecular doping: $Cr(CO)_3$ plus environment

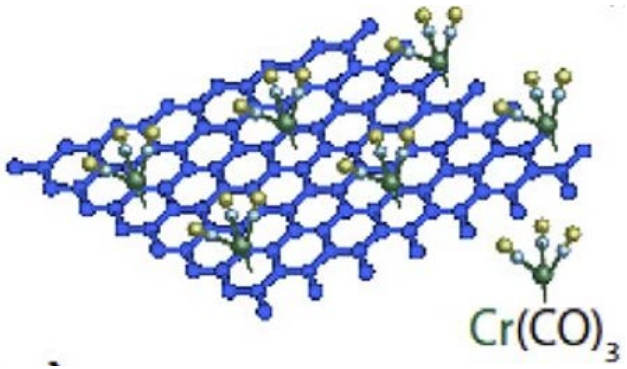

Chemical conversion from $Cr(CO)_6$
Ring-centered bonding /
Very small lattice distortion

Heating up to 110 °C removes most environmental dopants

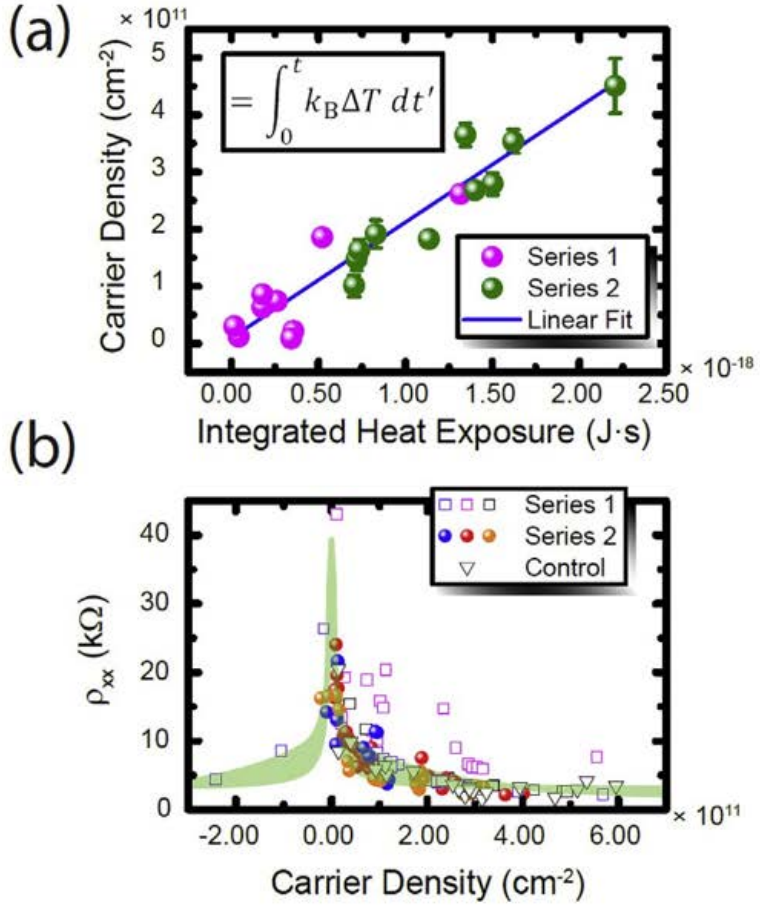

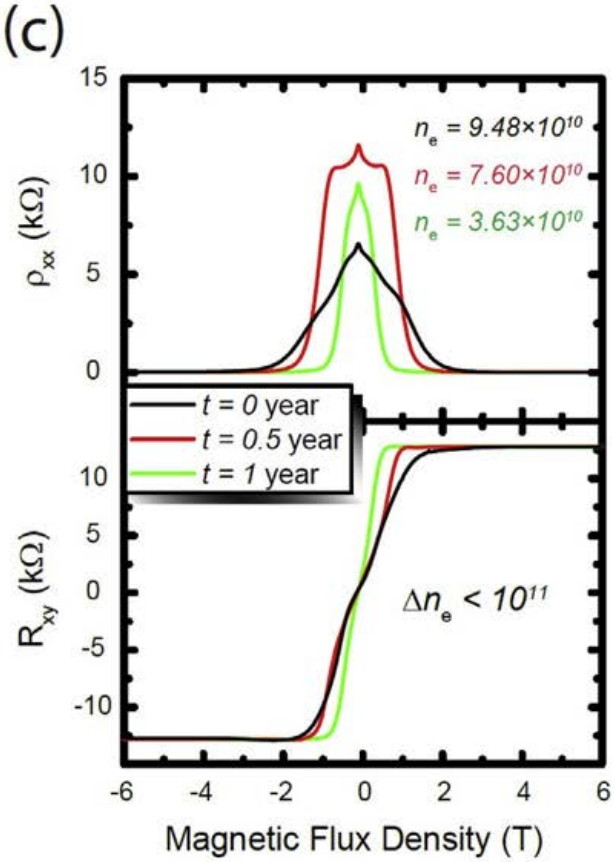

Series-parallel QHR arrays are like Wheatstone Bridges

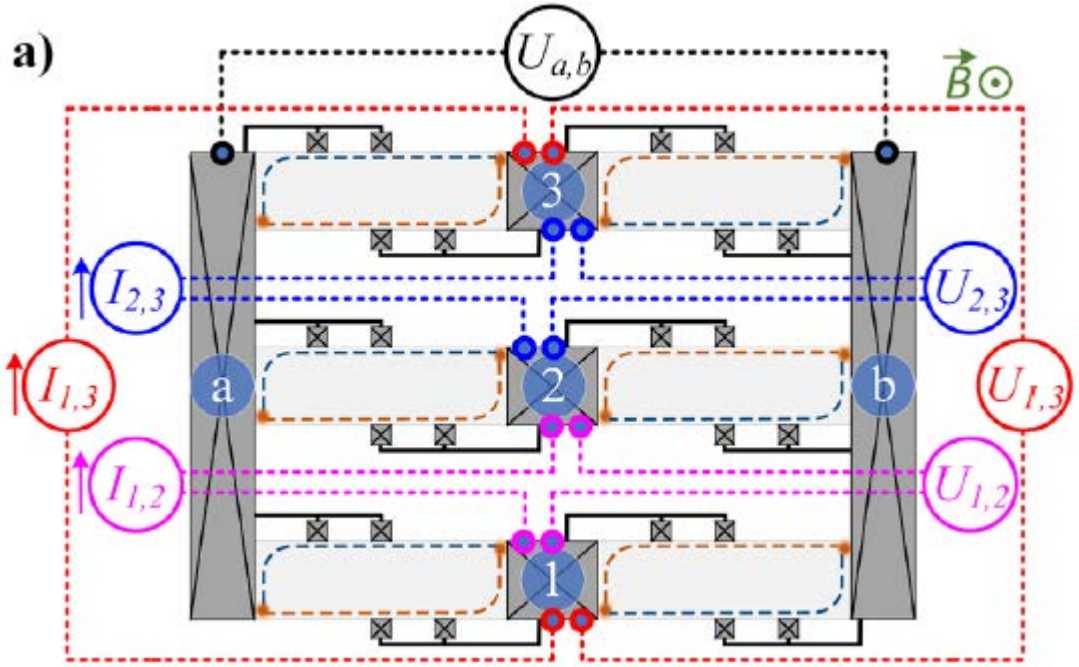

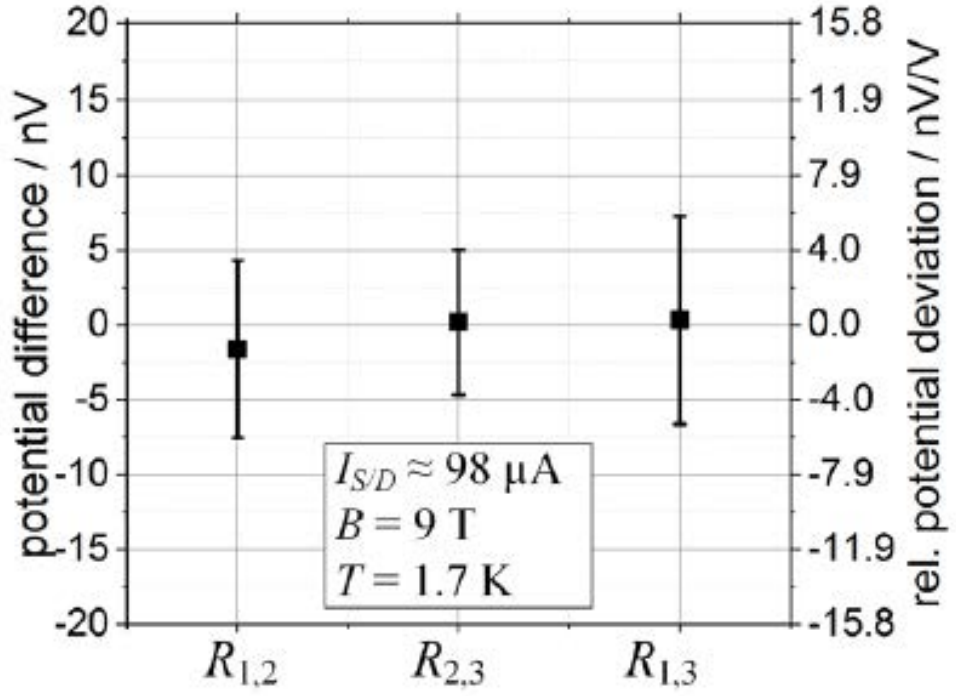

Quantization of any four of the six devices can be checked by injecting the test current at two of the midpoints (1, 2, 3) and measuring the voltage difference between points a and b.

Series-parallel QHR arrays are like Wheatstone Bridges – but may be complex

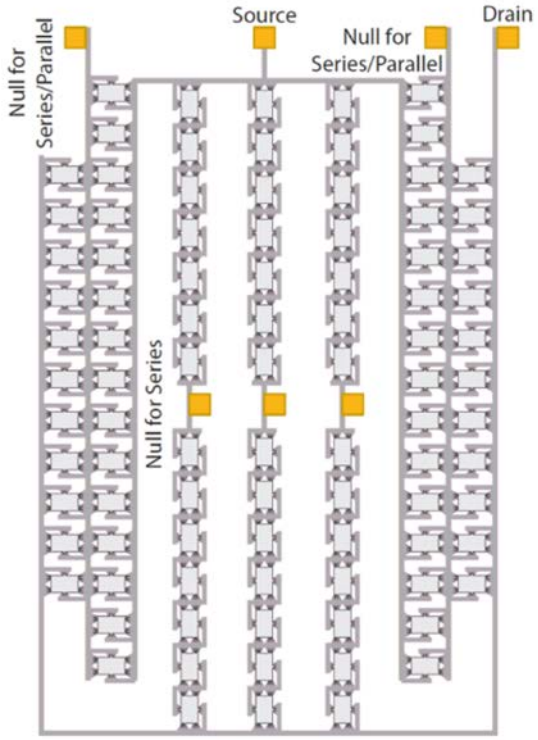

QHARS array of 94 QHR devices with symmetric Wheatstone bridge elements allows null voltage checks between intermediate contacts at similar voltage.

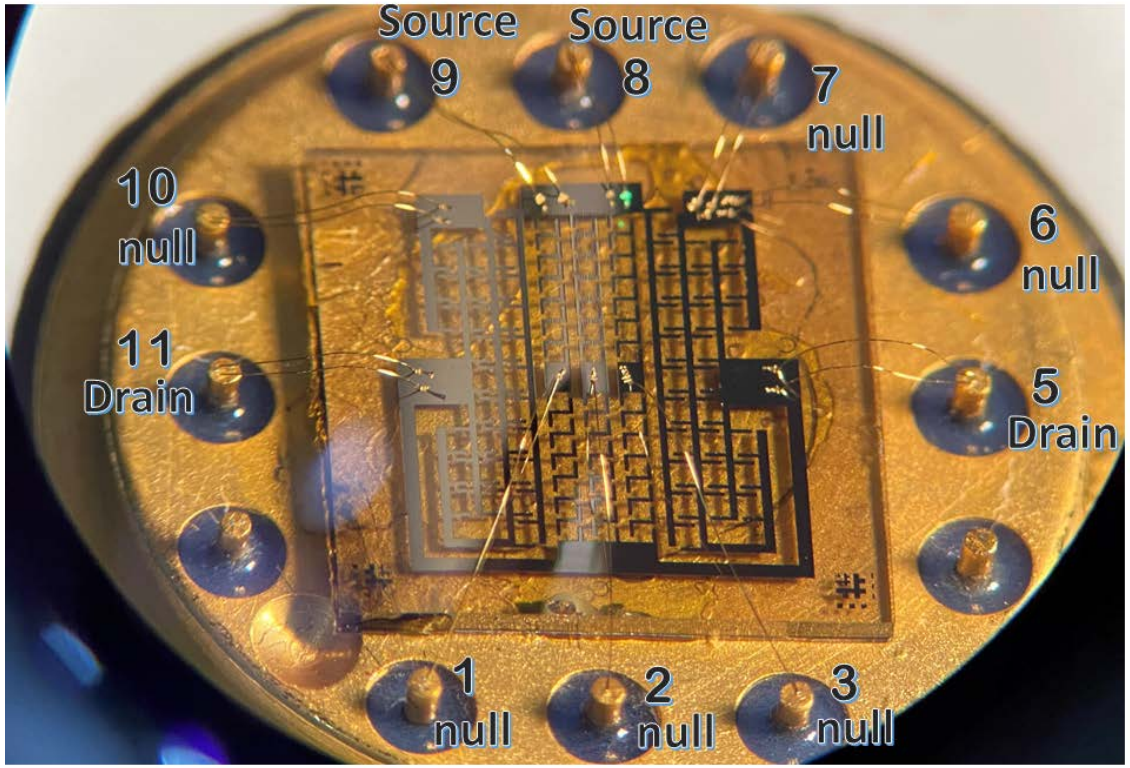

Full array quantized value = 999.985 304 Ω

NIST 992.8 Ω Graphene parallel array designs

Arrays feature NbTiN contacts and interconnections with 20 nm Au underlayer and branched source/drain contacts for reduced effective contact resistance. The superconductor transition occurs at 10 K – 12 K for all B-Fields up to 9 T.

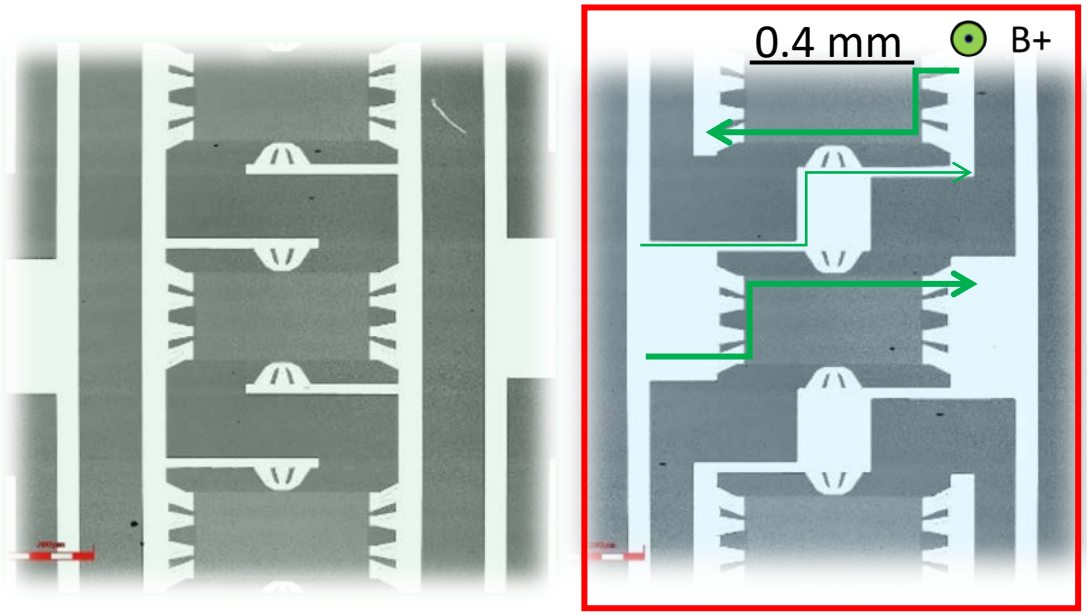

QHARS 13-device arrays. (a) Current flows in the same direction for all devices. (b) Current flows in alternating directions for adjacent devices to reduce capacitive losses between devices.

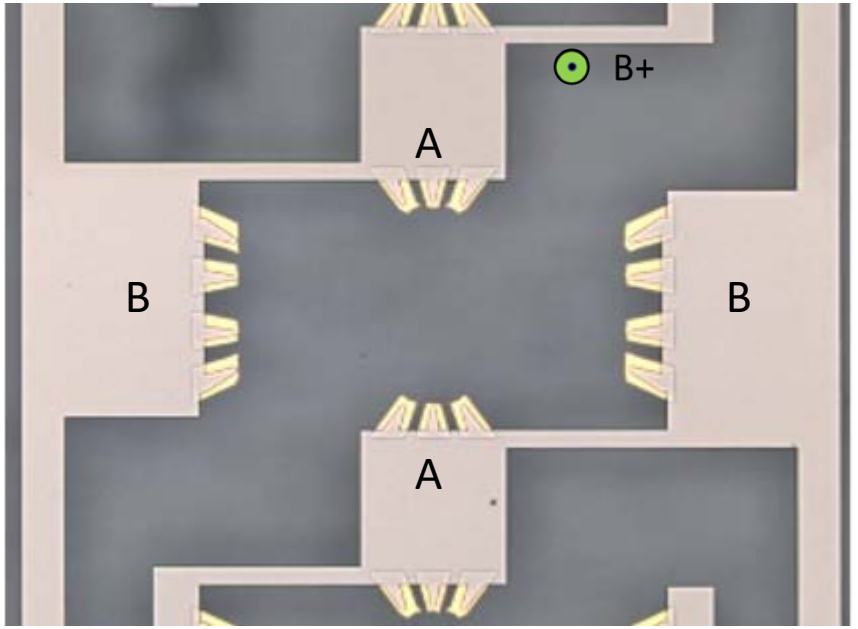

Single array element, showing

(A) voltage contacts

(B) source/drain with divided branches

M. Kruskopf *et al.*, "Next-generation crossover-free quantum Hall arrays with superconducting interconnections," *Metrologia*, vol. 56, no. 6, p. 065002, 2019.
M. Kruskopf *et al.*, "Two-terminal and multi-terminal designs for next-generation quantized Hall resistance standards: contact material and geometry," *IEEE Trans. Electron Dev.*, vol. 66, no. 9, pp. 3973 – 3977, 2019.

NIST 992.8 Ω Graphene parallel array designs

Contacts branched to minimize contact resistances.

B+

Opposing voltage contacts, small *Rxx component*

Typical Hall measurement, with opposing voltage contacts as-designed.

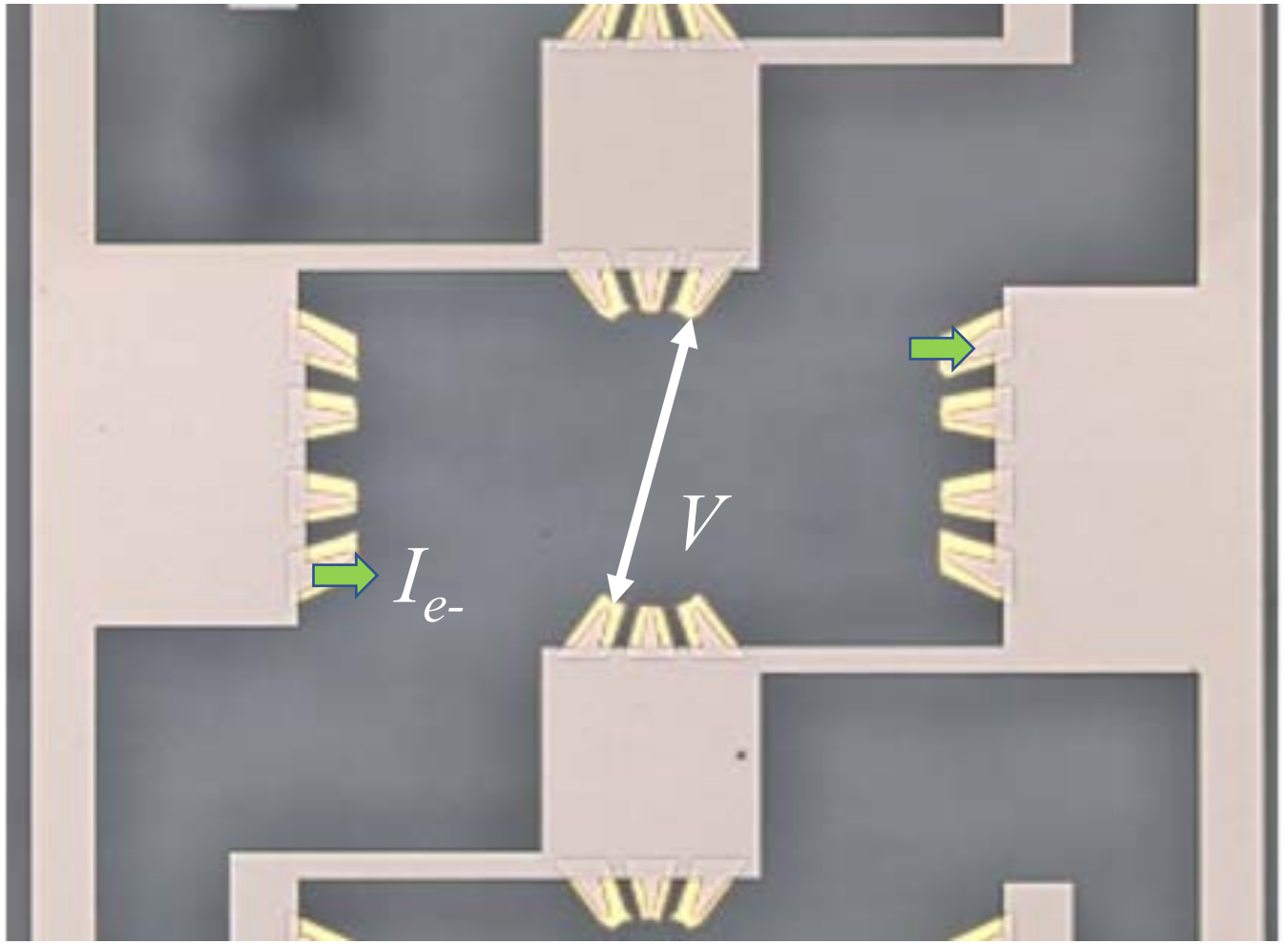

NIST 992.8 Ω Graphene parallel array designs

Contacts branched to minimize contact resistances.

B+

Opposing voltage contacts, small *Rxx* component

B-

Diagonal voltage includes larger *Rxx* influence

Reverse-field measurement, with voltage contacts misaligned.

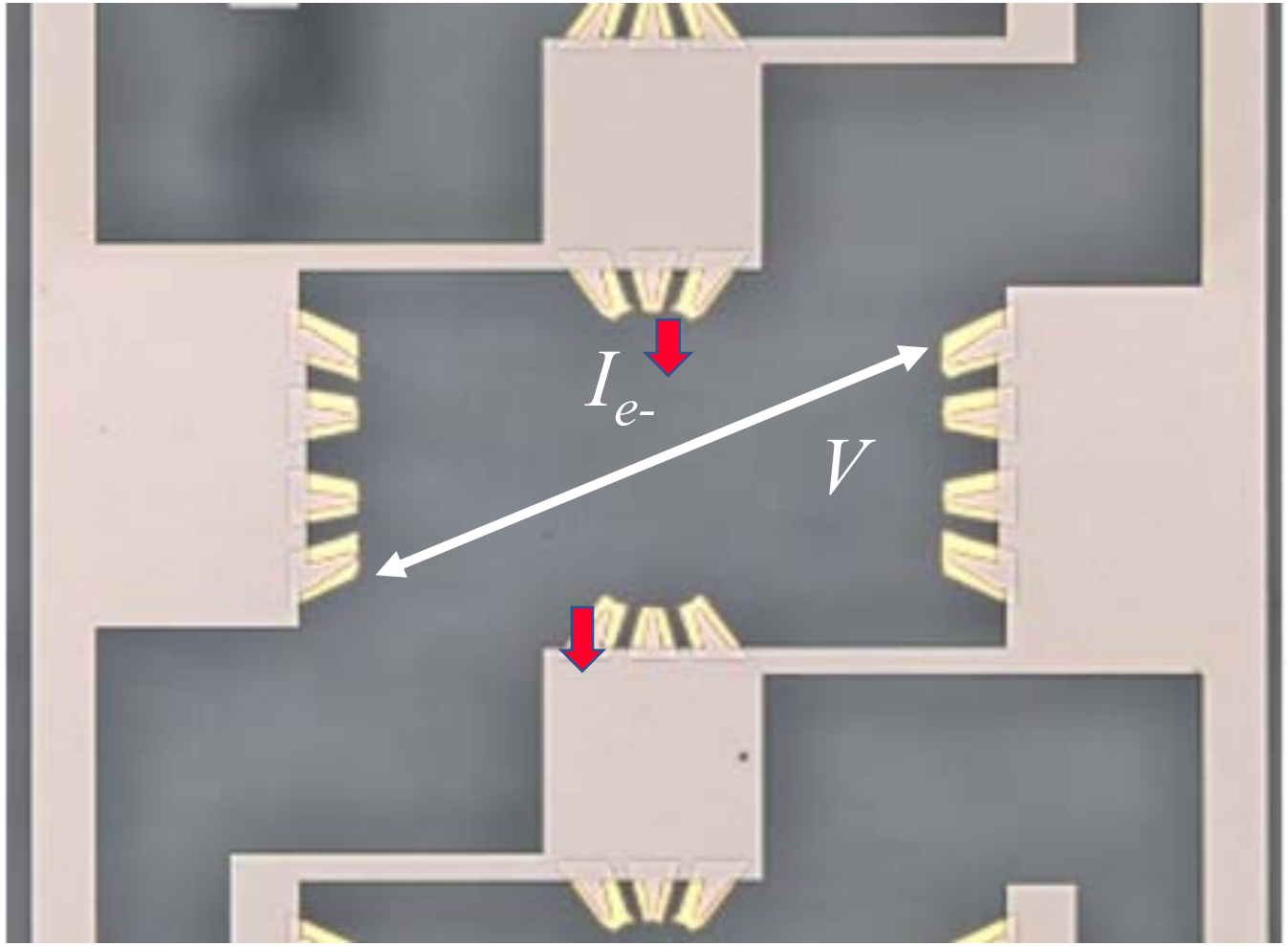

ONSAGER-CASIMIR FRUSTRATION FROM RESISTANCE …

PHYSICAL REVIEW B **104**, 085418 (2021)

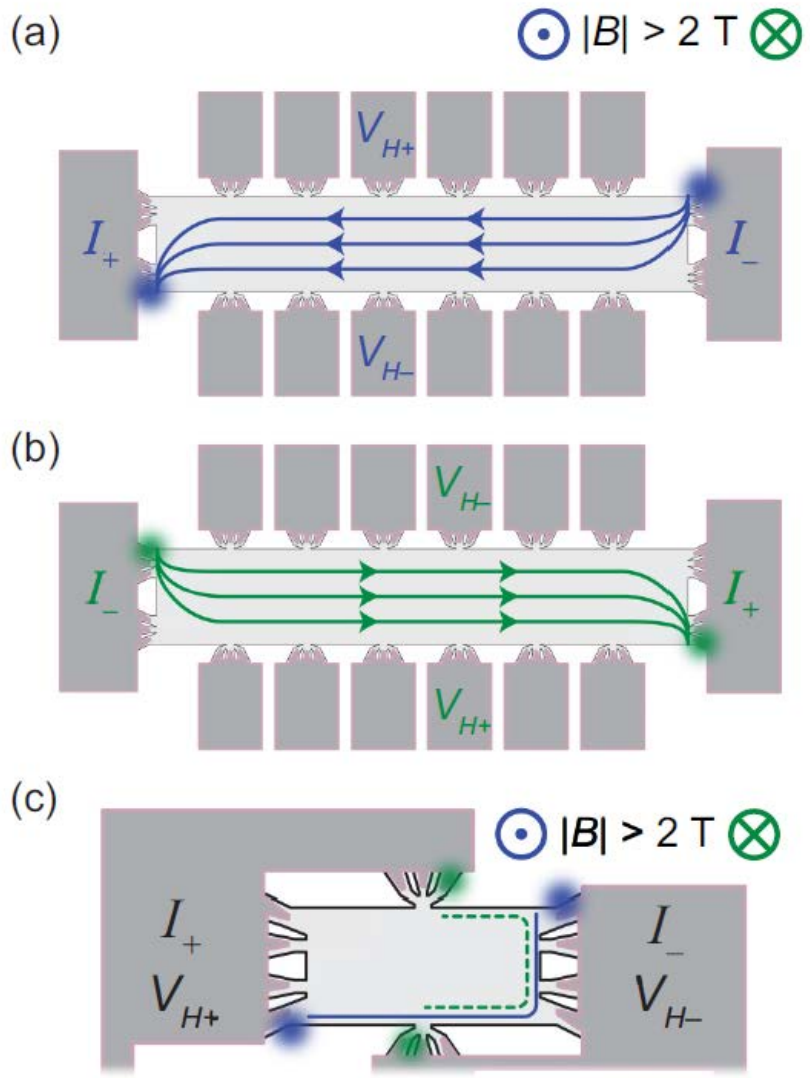

Before QHR array devices are globally implemented as standards, it is critical to disseminate best practices for characterization of the Hall resistance quantization for *B* field and current dependence.

The symmetry of electrical conductance for opposite perpendicular directions of *B* field is one such criterion, as a result of the well-known Onsager-Casimir relations (OCRs):

$$R_{12,34}(B+) = R_{34,12}(B-)$$

$I \quad V$ $\qquad$ $I \quad V$

Onsager-Casimir Reciprocity
1) Reversal of magnetic field
2) Interchange of source and detector

OCR typically holds at low field (B ≈ 0); always holds on a quantized QHR plateau.

Fails for transition region, because of substrate disorder and carrier dynamics.

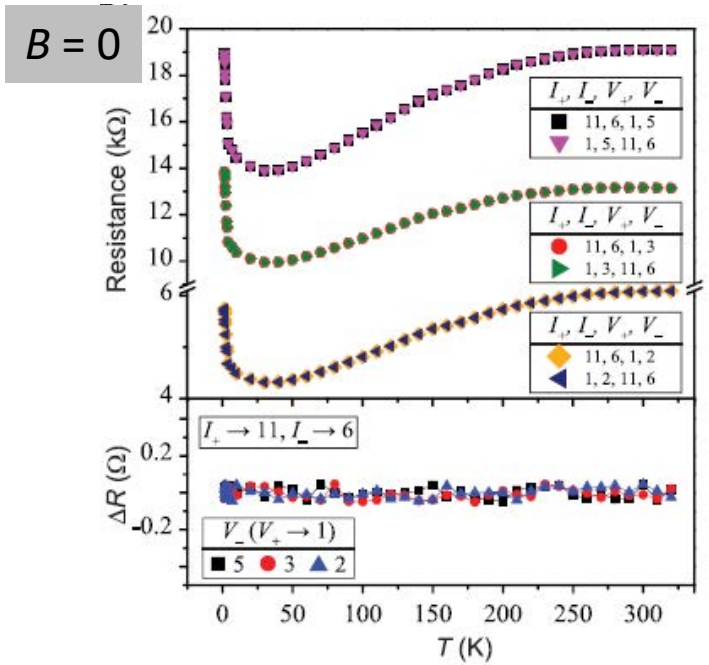

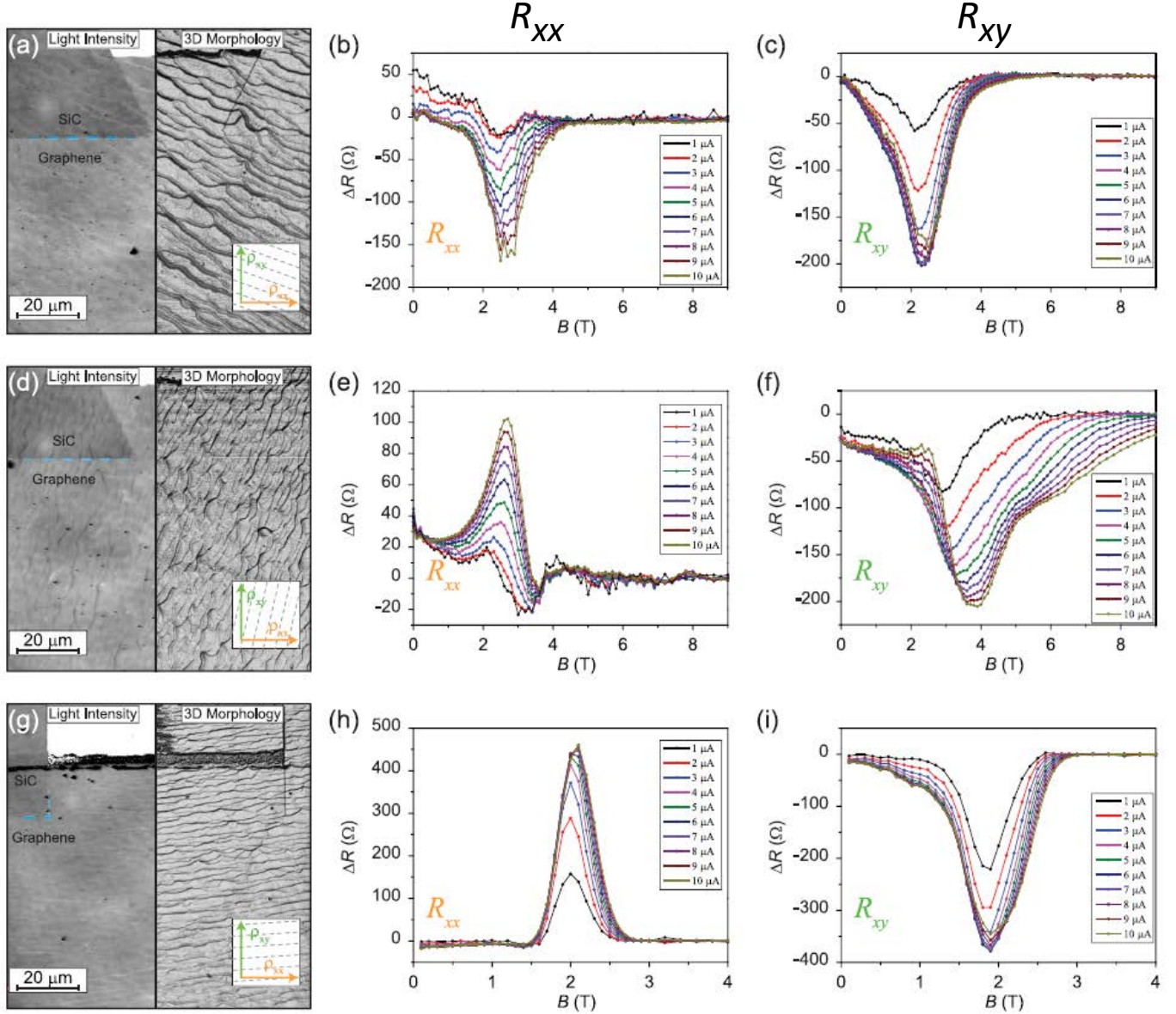

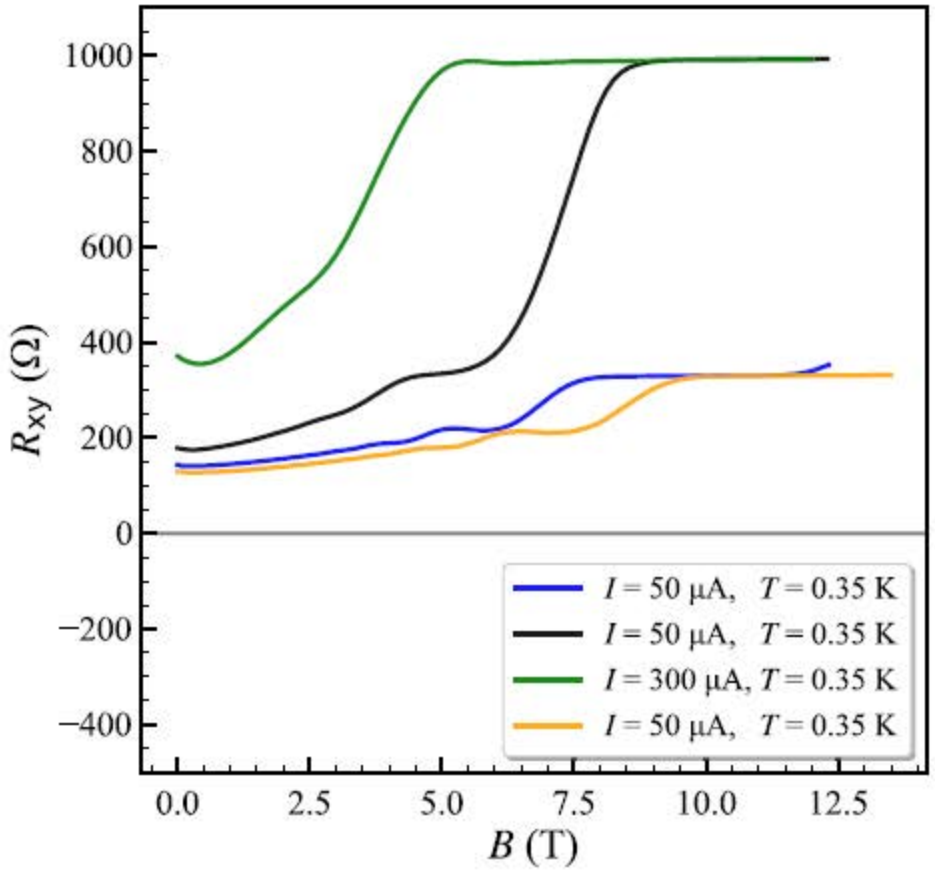

FIG. 5. Measured QHARS resistance using a current source and digital voltmeter, for several carrier density levels (n_0). Starting with the highest resistance at $B = 0$ (green), heating in vacuum was used to increase n_0 to around 7×10^{11} cm^{-2} (black). Subsequent heating cycles in vacuum were used to produce the blue curve with $n_0 \approx 1.6 \times 10^{12}$ cm^{-2} (not discussed in the text), and the yellow curve with $n_0 \approx 1.7 \times 10^{12}$ cm^{-2}, where a broad plateau is observed near 330.93 Ω.

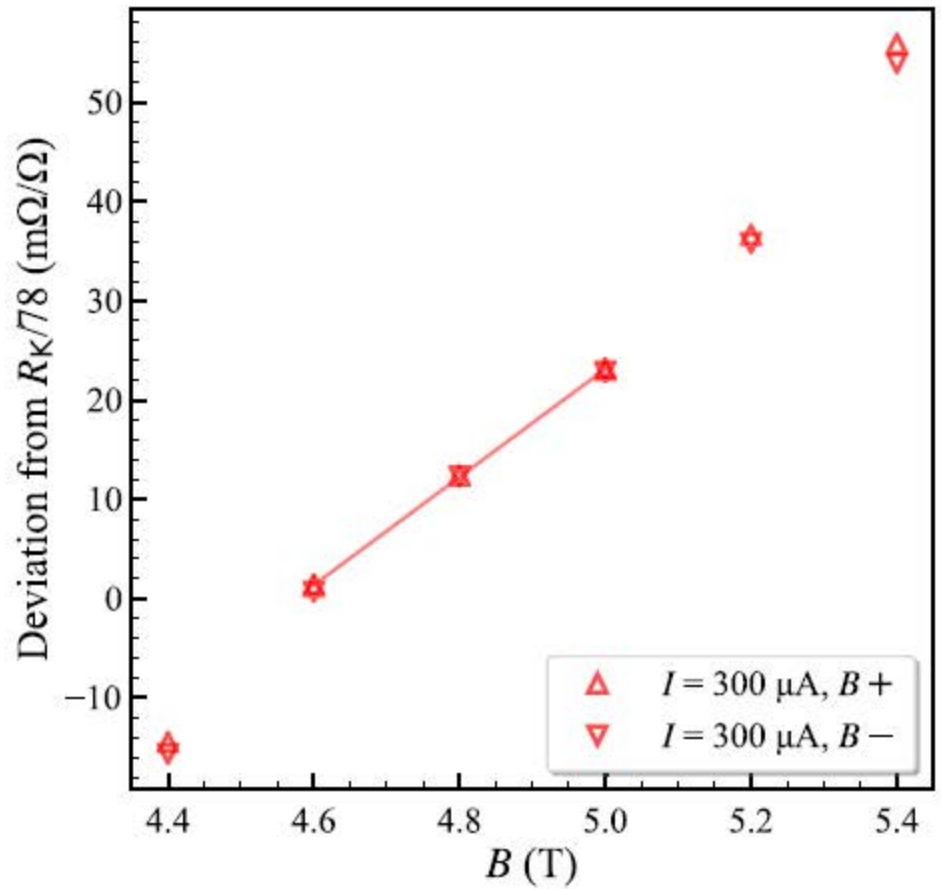

FIG. 6. The region near 330.93 Ω for the black curve of Fig. 5, with $n_0 \approx 7 \times 10^{11}$ cm^{-2}. The $\nu = 6$ plateau is not visible, but these points show the minimum slope region measured using the DCC bridge at resistance levels near $R_K/78$. The slope of the fitted line is ≈54.5 (mΩ/Ω)/T and the plateau center was estimated as $B \approx 4.8$ T.

NIST QHARS Arrays Characterized at $h/78e^2 \approx 330.93\ \Omega$

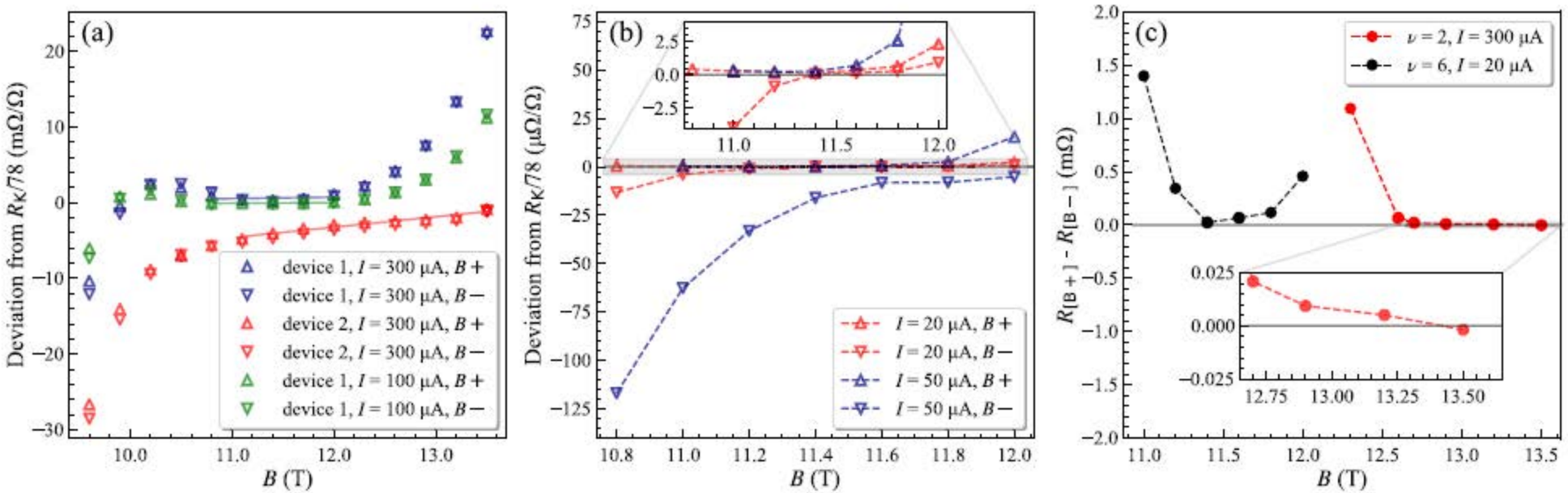

FIG. 8. Resistance quantization measurements for device 1 at $T \approx 0.35$ K. Standard deviations are smaller than the size of the markers, as derived from DCC bridge ratios. (a) The $B+$ and $B-$ resistance for the $\nu = 6$ plateau near $R_K/78 \approx 330.933\,429\ \Omega$, where fitted lines are offset from the quantized value over a range of 1 T, with the scale in mΩ/Ω. (b) The $\nu = 6$ resistance differs from the quantized value by $(0.247 \pm 0.054)\ \mu\Omega/\Omega$ for $I = 20\ \mu$A and by $(0.402 \pm 0.027)\ \mu\Omega/\Omega$ for $I = 50\ \mu$A over a range of 0.6 T in $B+$, from 11 to 11.6 T; the scale is in $\mu\Omega/\Omega$. For the plateau center of 11.2–11.4 T, the measured deviation is $(0.171 \pm 0.076)\ \mu\Omega/\Omega$ at 20 μA and $(0.264 \pm 0.078)\ \mu\Omega/\Omega$ at 50 μA. The expanded uncertainties are for a 2σ confidence interval. (c) Comparing the magnetic field reciprocity at the $\nu = 2$ and 6 filling factors.

Realization of Mass with the Kibble (Watt) Balance

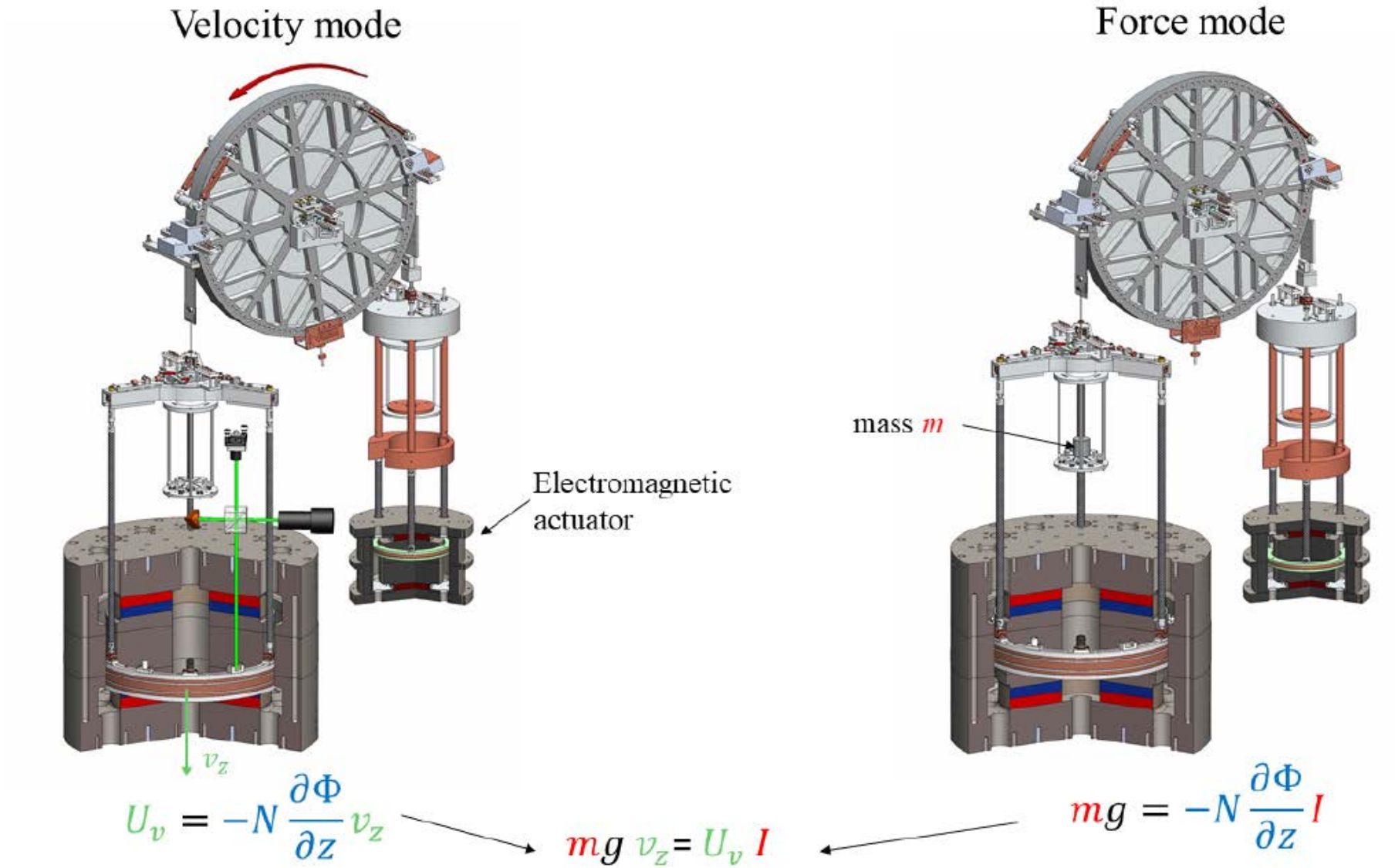

Velocity mode: Measure moving coil velocity (v_z), voltage (V)

Programmable Josephson voltage standard used for quantized voltage

Force mode: measure current (I) needed to support mass on stationary coil

Quantum Hall array standard used as reference for measuring the current

100 g mass = m

Laser interferometer – v_z

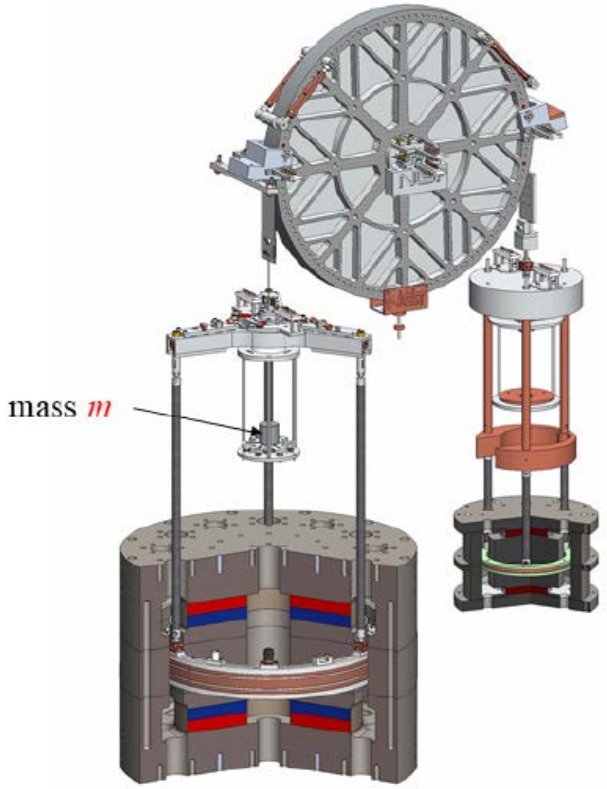

$$mg\ v_z = U_v\ I$$

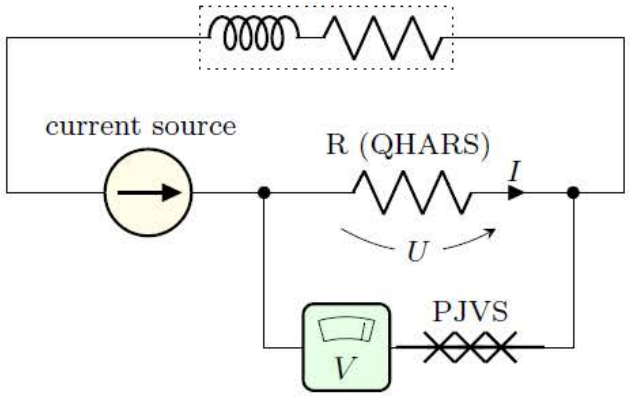

FIG. 1: Simplified electrical circuit of the NIST Kibble balance coil connected directly to two quantum electrical standards. The programmable Josephson voltage standard (PJVS) is adjusted until the voltage measured is almost zero to achieve the lowest uncertainty.

Realization of 100 g Mass with the Kibble (Watt) Balance requires precise current near 0.7 mA

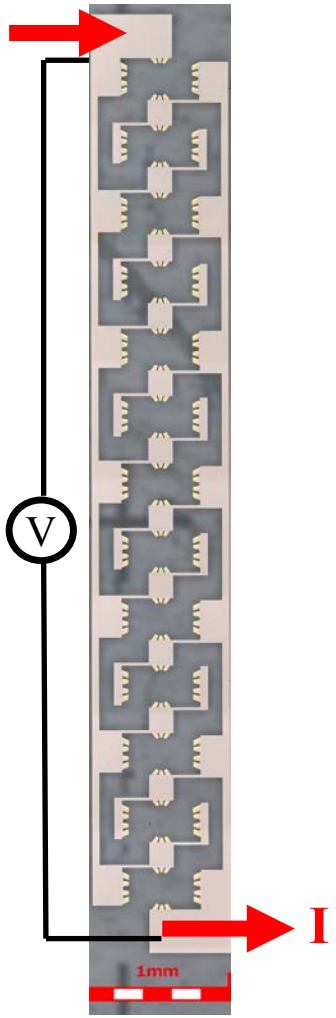

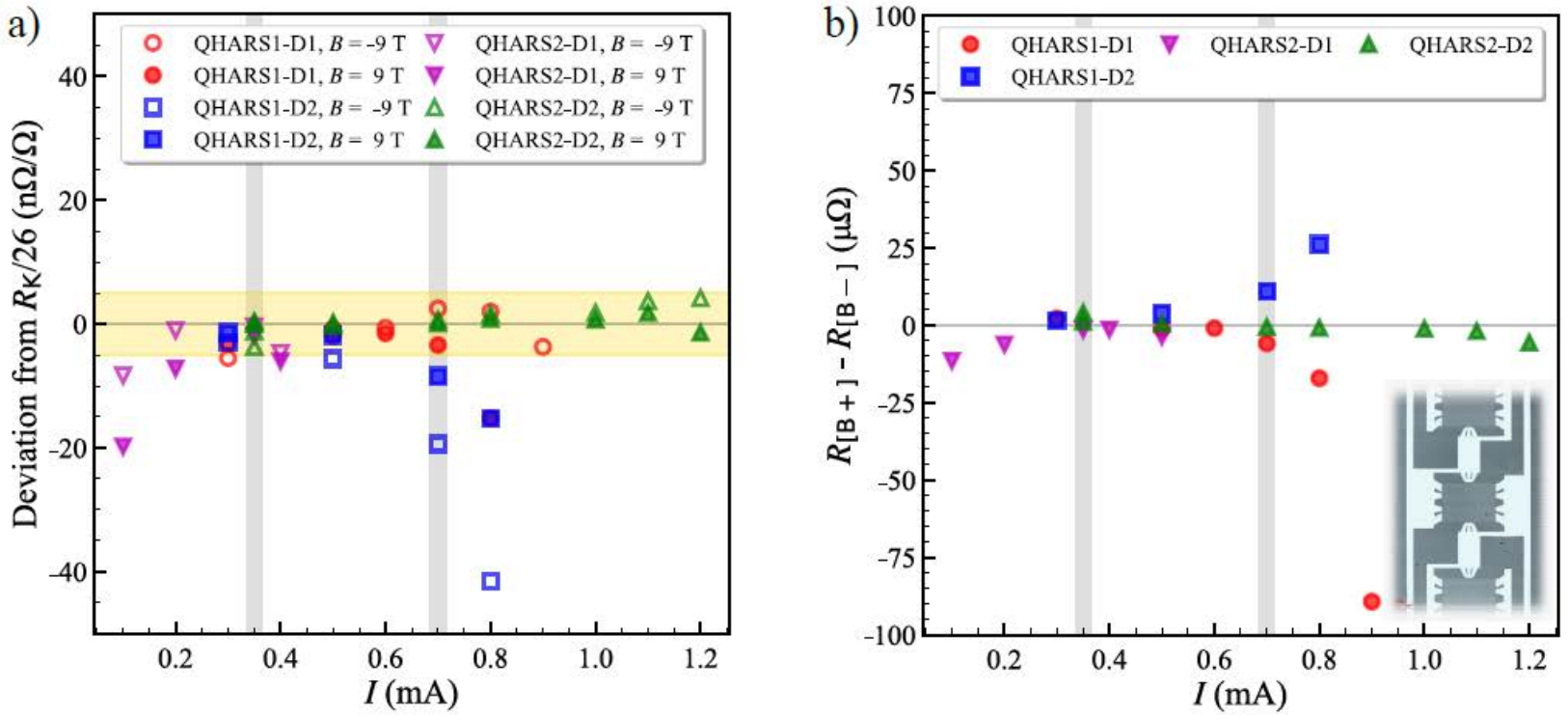

FIG. 2: Cryogenic current comparator bridge (CCC) measurements for four QHARS devices (QHARS1-D1, QHARS1-D2, QHARS2-D1, and QHARS2-D2) at $T = 1.6\,\mathrm{K}$ and $|B| = 9\,\mathrm{T}$. The plot on the left shows the deviation of the measured resistance of QHARS devices from the nominal value of $R_\mathrm{K}/26$ as a function of source-drain current [24, 25]. The QHARS devices were used at 0.35 mA and 0.7 mA (grey bands) to measure 50 g and 100 g masses where they showed excellent quantization. The plot on the right shows magnetic field reciprocity measurements for the four QHARS devices as a function of source-drain current.

A Macroscopic Mass From Quantum Behavior In An Integrated Approach, F. Seifert, *et al.*, in preparation 2022

Realization of Mass with the Kibble (Watt) Balance

Source-Drain current = 0.7 mA
QHARS T = 1.6 K and $|B|$ = 9 T
Uncertainty = 12.8×10^{-9}

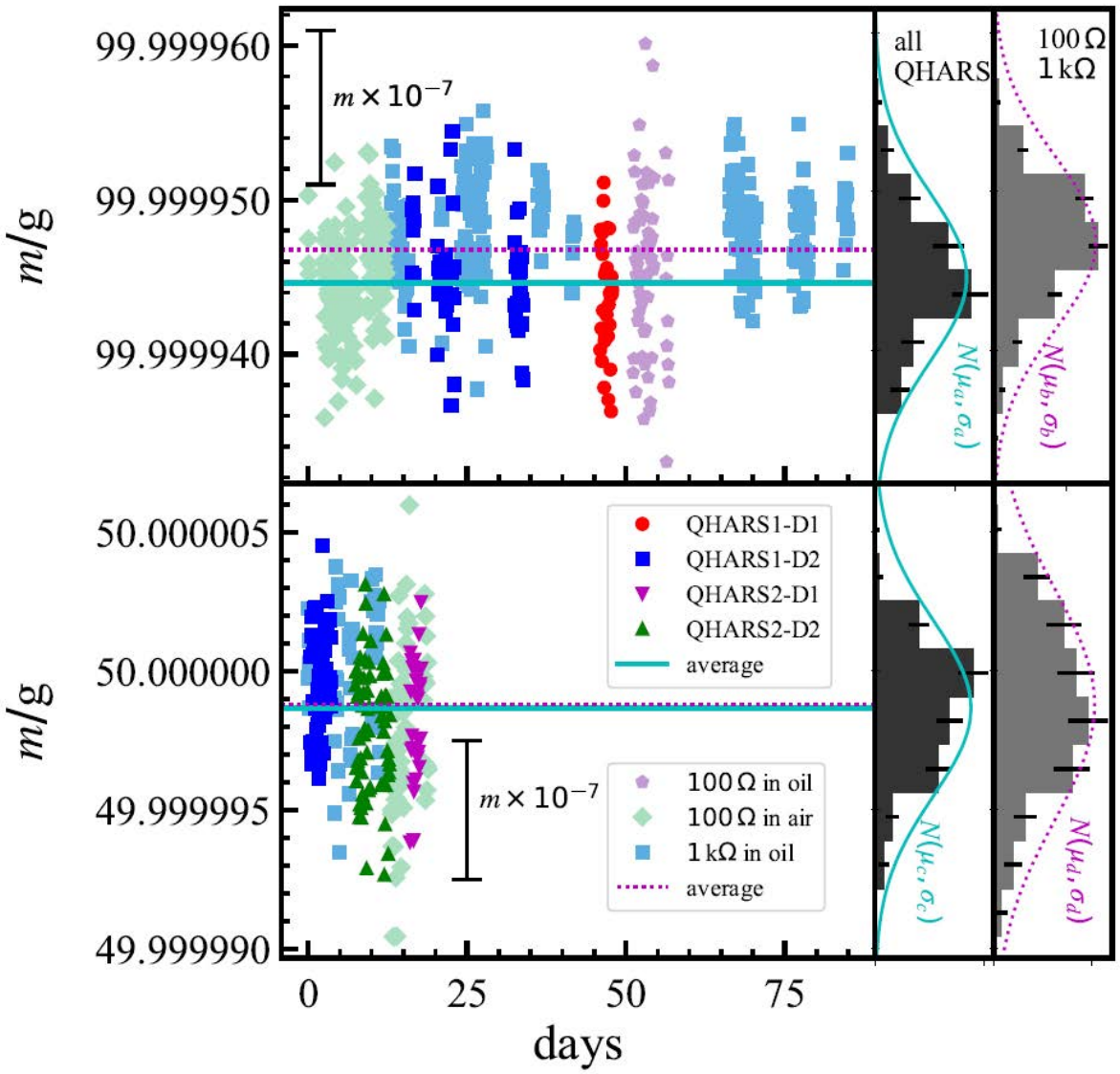

100 g mass

Source-Drain current = 0.35 mA
QHARS T = 1.6 K and $|B|$ = 9 T
Uncertainty = 20×10^{-9}

50 g mass

Quantum Metrology Triangle completed!

NIST

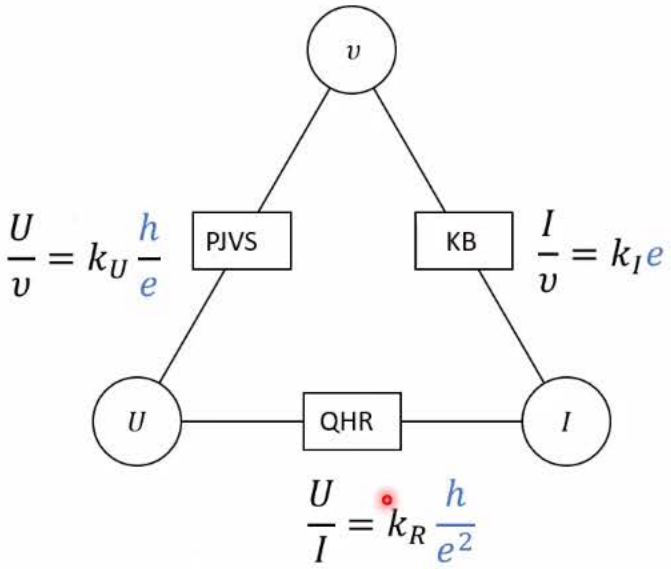

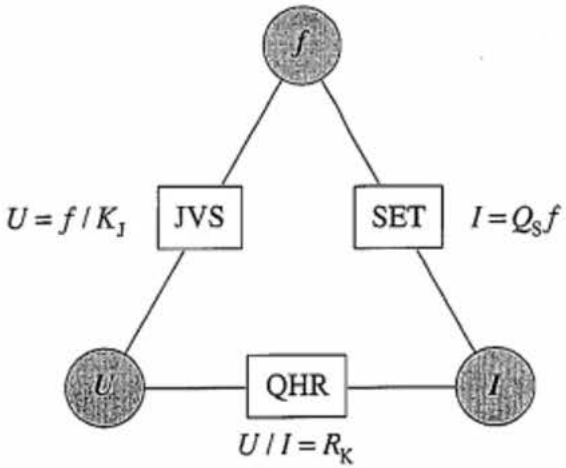

Figure 1. Original version of the QMT proposed in 1985 [3]. It links the Josephson effect (JVS), the quantum Hall effect (QHR) and the single-electron tunnelling effect (SET) by using Ohm's law.

Keller M., *Current Status of the quantum metrology triangle*, Metrologia **45** (2008) 102-109

Graphene quantized Hall array of 101 elements used as a 33.6 MΩ Wye-Delta device

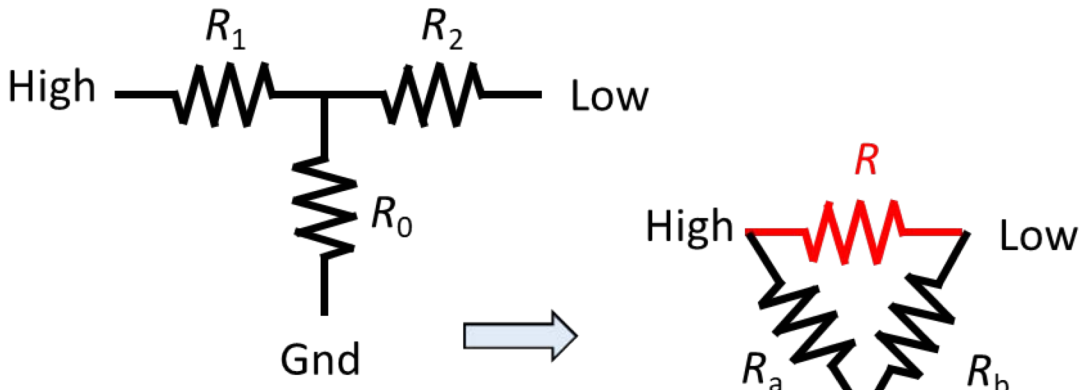

$$R = (R_1 \times R_2) / R_0 + R_1 + R_2$$

Wye and delta configurations of a resistor network. The formula defines the value R from the R_1, R_2, and R_0 sections of the wye network. R_a and R_b are the leakage resistances, negligible at these resistance levels.

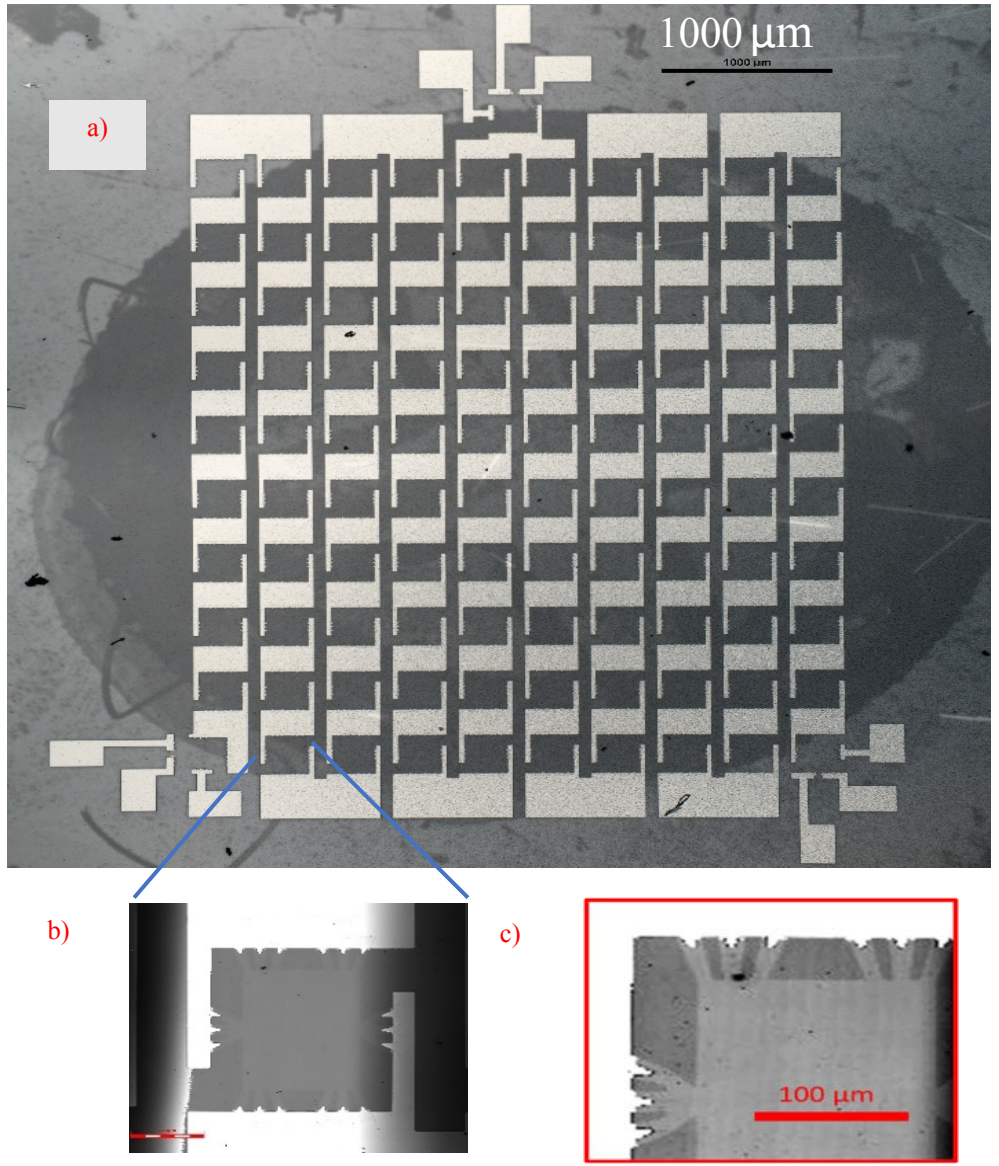

Graphene Quantized Hall Arrays as Wye-Delta Transfer Standards, D. G. Jarrett, submitted abstract, CPEM 2022

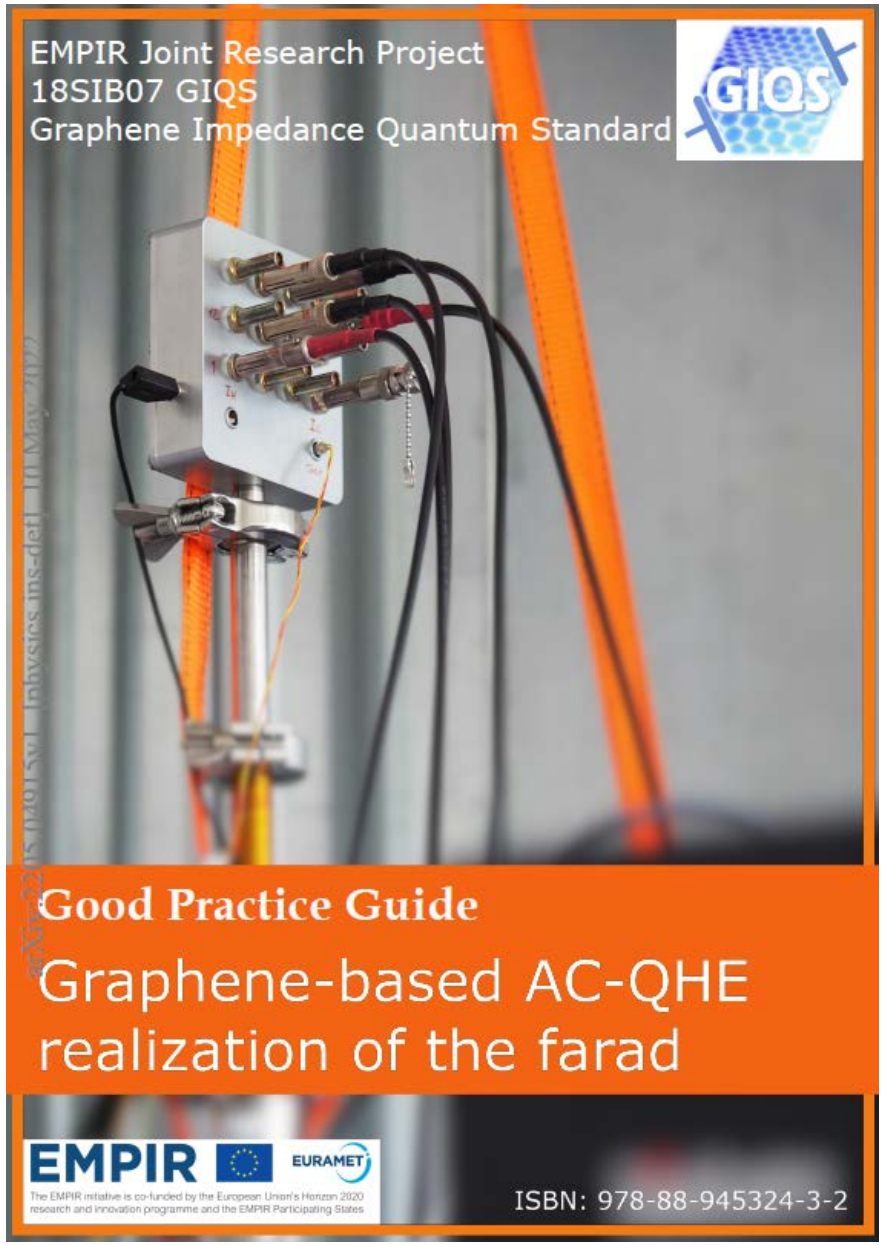

L. Callegaro, *et al.*, arXiv:2205.04915v1

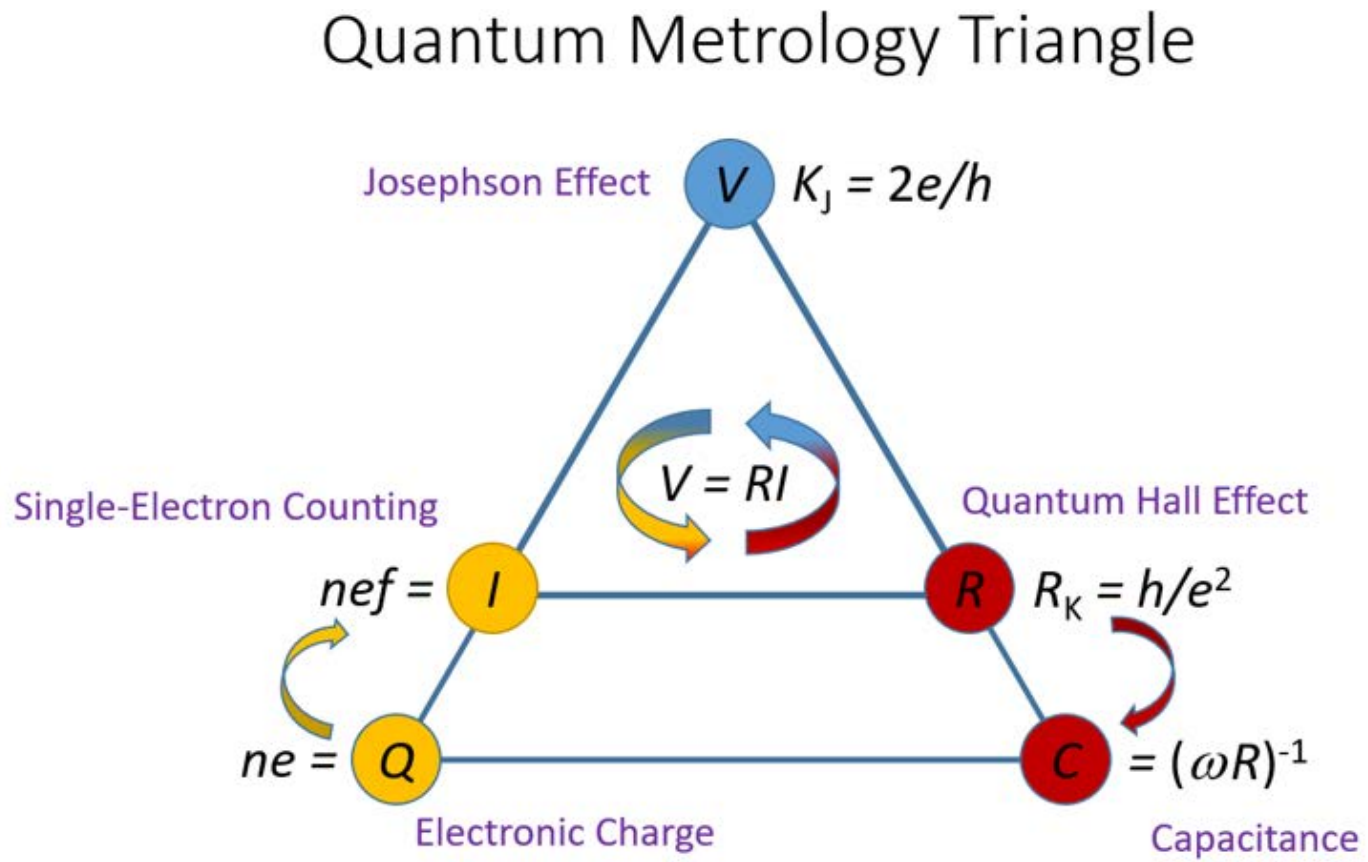

Development of AC QHR digital bridge linking the Farad to the SI

Figure 5.1: Traceability chain for the realisation of capacitance (at 10 pF – 100 pF level)

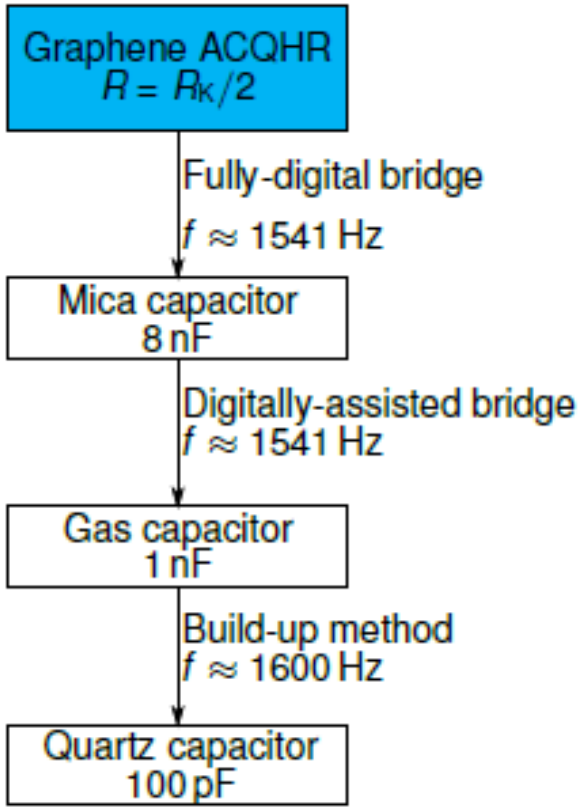

Figure 5.2: Traceability chain under development at INRIM (Italy) the AC QHR in graphene

L. Callegaro, *et al.*, arXiv:2205.04915v1

National Institute of Standards and Technology
U.S. Department of Commerce

UNIVERSITY OF MARYLAND

GRAPHENE WAVES

國立臺灣大學
National Taiwan University

PTB Physikalisch-Technische Bundesanstalt
Braunschweig and Berlin
National Metrology Institute





NIST Epitaxial Processing

- **Concentration of Si-vapor**
  (Facing Graphite surface)

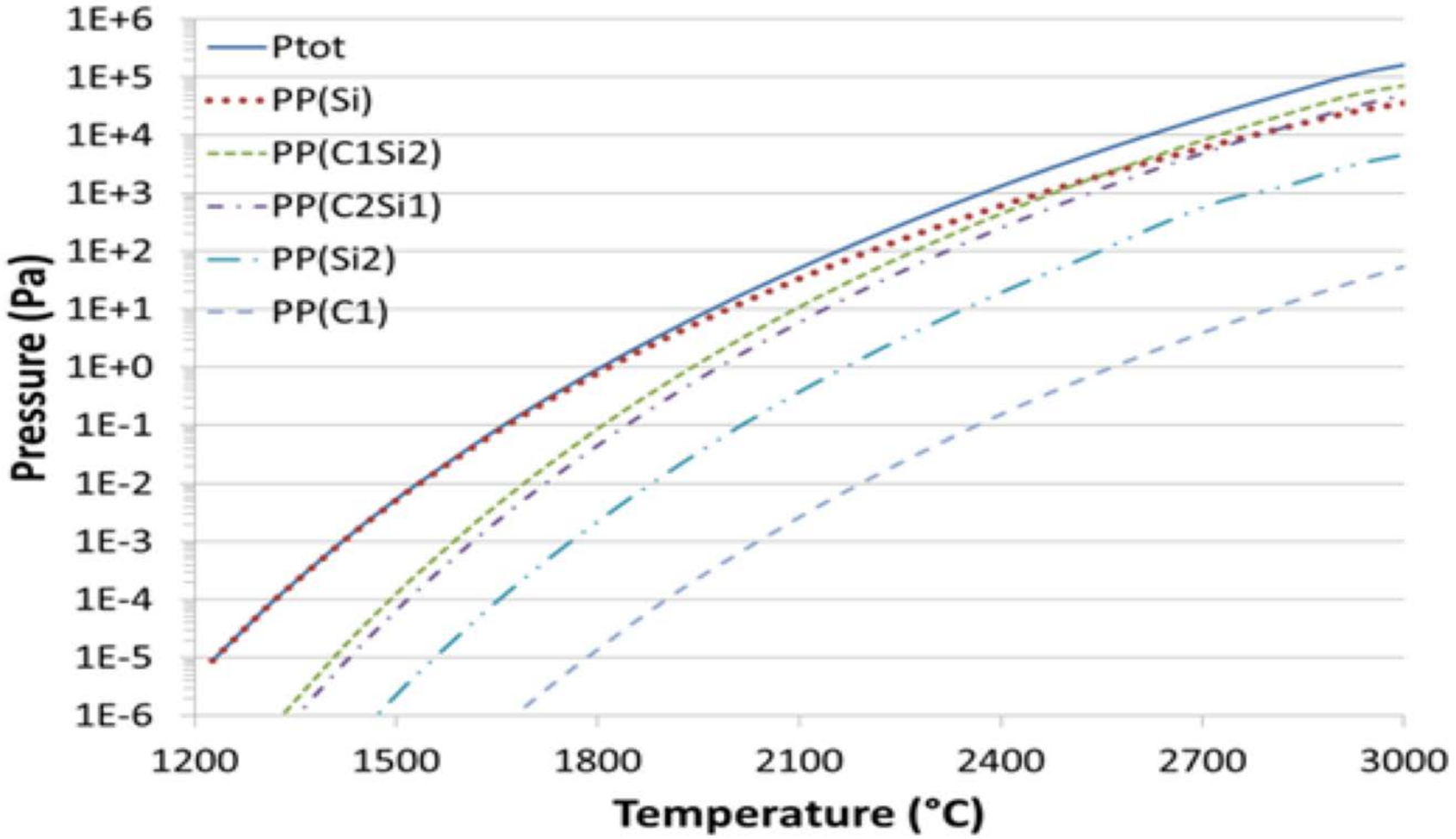

NIST 992.8 Ω QHARS Graphene Array: Device 2, 9 T system (1.6 K)
CCC bridge comparisons based on selected 100 Ω standards

DCC bridge measurements from 100 Ω

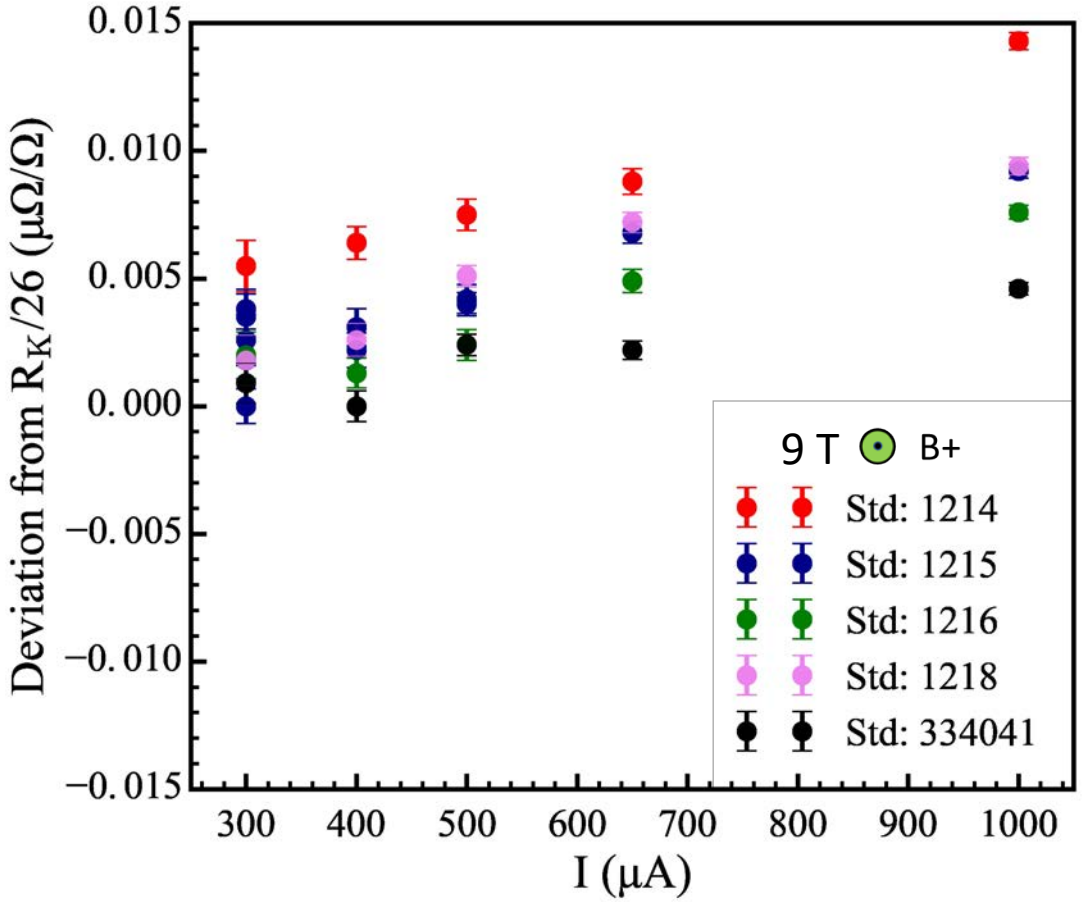

DCC calibration against CCC bridge

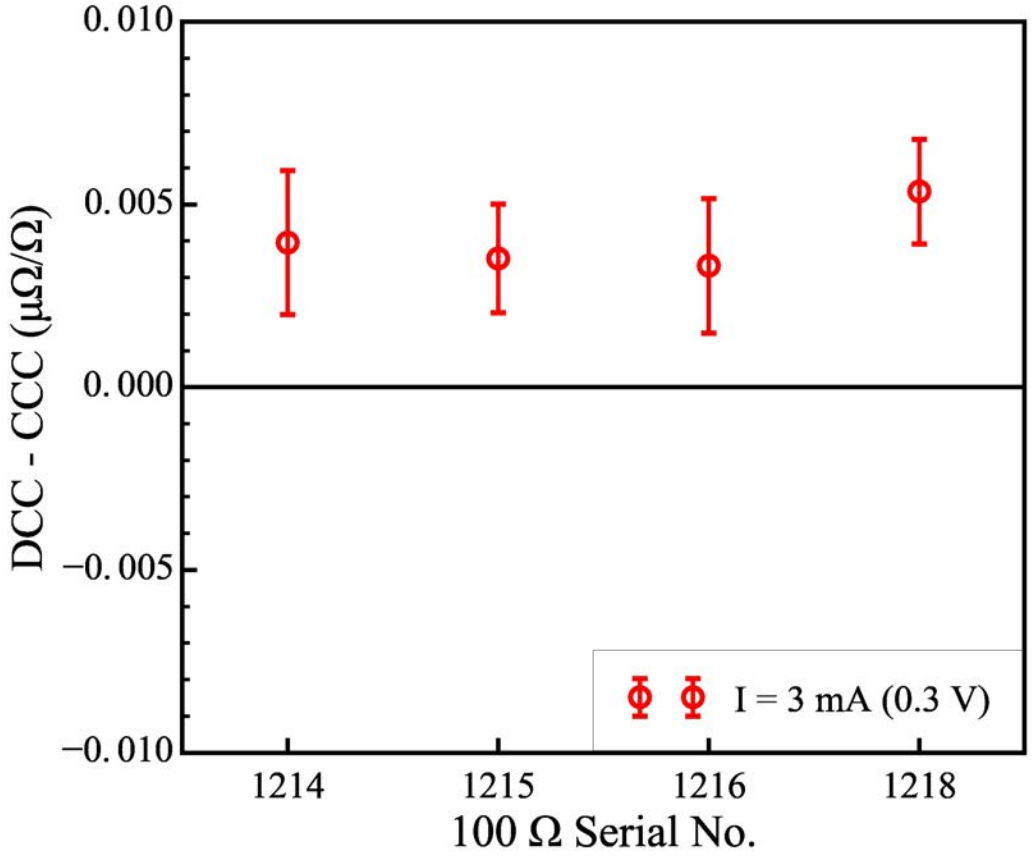

NIST Epitaxial Processing

Hole-type molecular doping

(a) AFM image before fabrication.
(b) Longitudinal resistivity and Hall resistance measured one week (dashed lines) and one month (solid lines) after the fabrication, respectively at 4.3 K.
(c) Temperature dependence of the carrier density and mobility measured one week (dashed) and one month (solid) after fabrication.

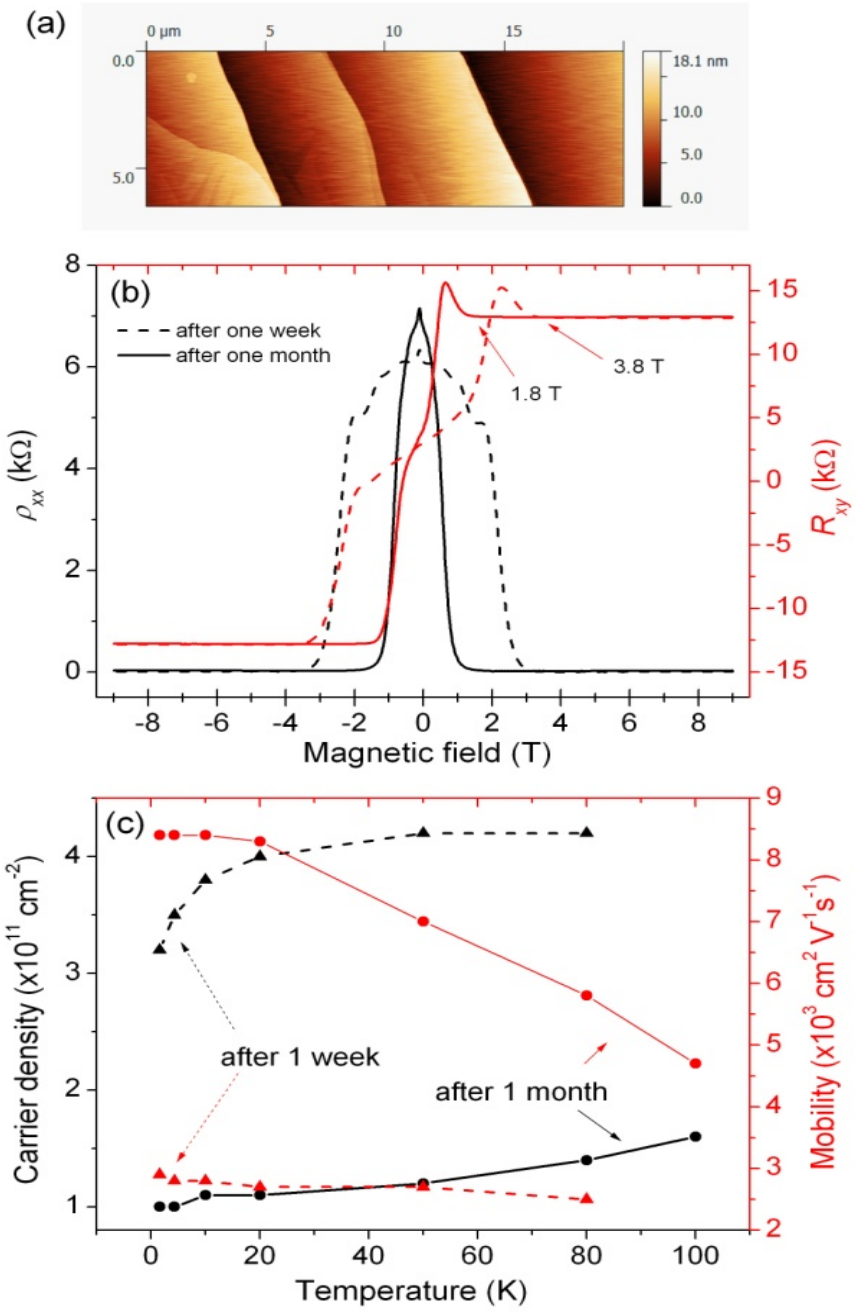

Molecular doping: $Cr(CO)_3$ plus environment

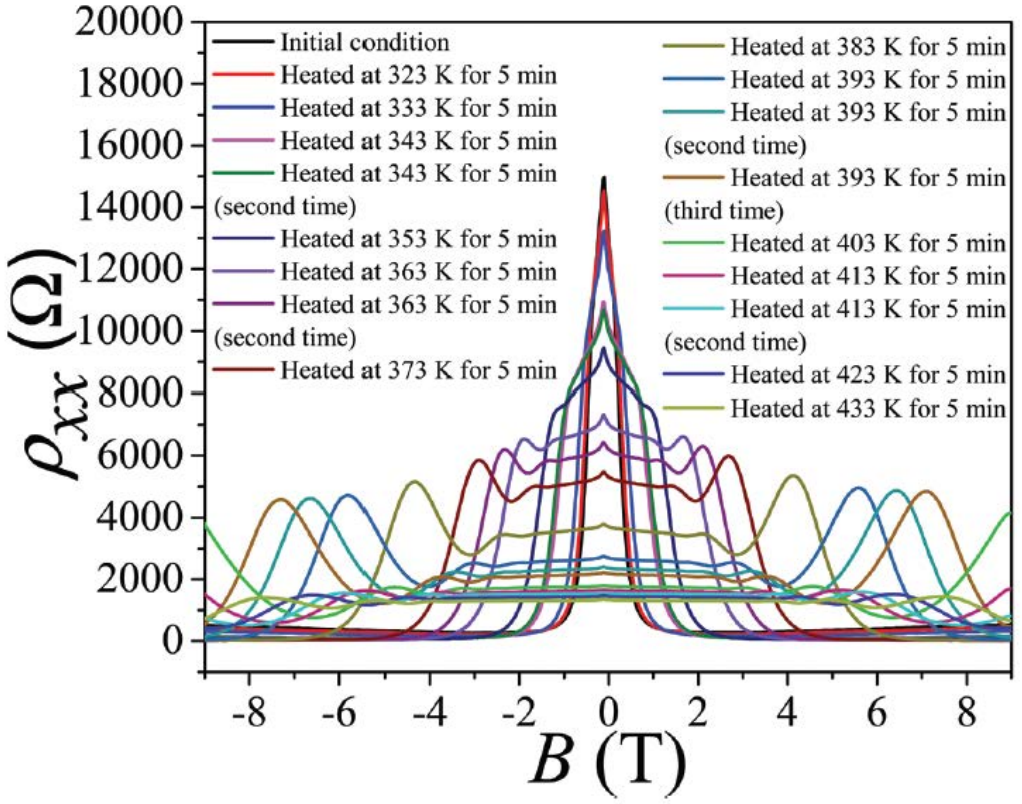

Chiashain Chuang, et al., Nanoscale, 9, 11537 (2017)

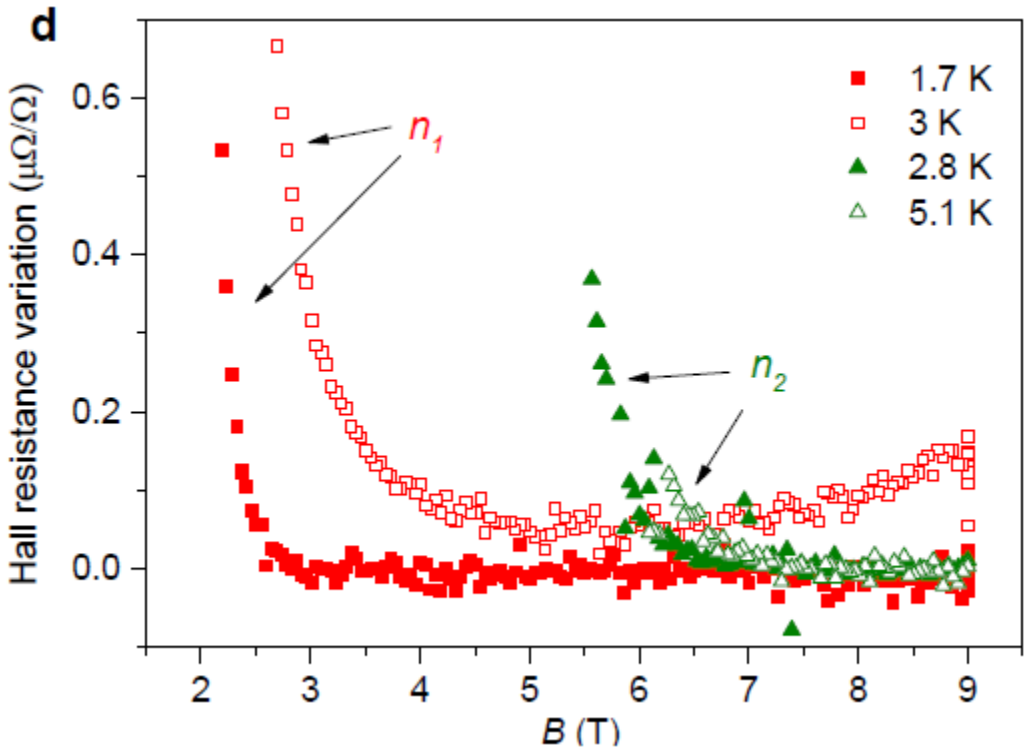

Epitaxial graphene homogeneity and quantum Hall effect in millimeter-scale devices, Yanfei Yang, *et al*. Carbon 115 (2017)

Confocal Laser Scanning Microscopy (CLSM):

Scan focused 405 nm laser beam in XY plane

Photomultiplier collects confocal reflected light

Intensity data is plotted for range of focal planes

Image contains Z-position data

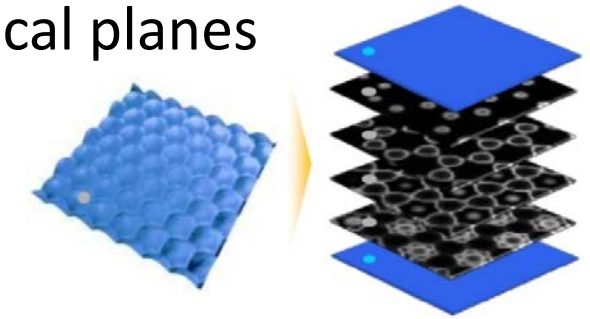

A circular pinhole is used to remove out of focus data.

Only in focus light is acquired.

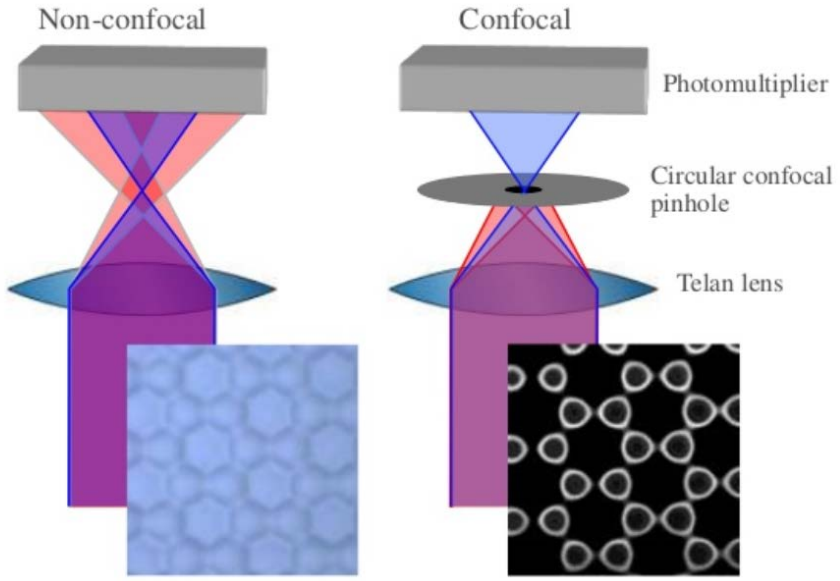

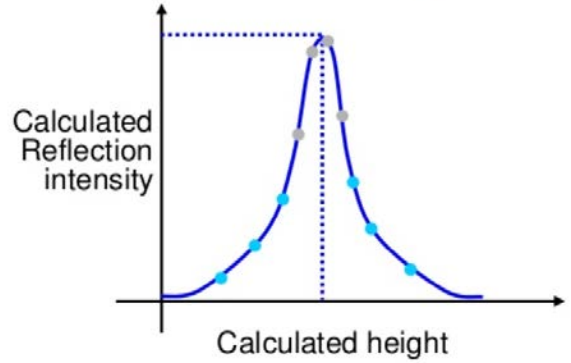

Variation in intensity is measured at each image pixel.

Multiple of points located in the proximity of the point with the highest intensity are extracted.

The curve of an ideal I-Z curve is calculated.

Graphene with superconducting interconnects for quantum Hall arrays

Elmquist R [1] , Kruskopf M [1,2*] , Patel D [1,3] , Liang C [3]
[1] *National Institute of Standards and Technology, Gaithersburg, MD 20899-8171*
[2] *Joint Quantum Institute, University of Maryland, College Park MD, 20742*
[3] *Department of Physics, National Taiwan University, Taipei 10617, Taiwan*
** Present address: Physikalisch-Technische Bundesanstalt, Bundesallee 100, D-38116 Braunschweig*

Resistance arrays based on multiple quantum Hall effect (QHE) devices often suffer from accumulated resistance errors from contacts and interconnections. In this work we describe Quantized Hall Array Resistance Standards (QHARS) constructed with NbTiN superconducting contacts and monolayer epitaxial graphene (EG). We also introduce symmetric-array designs with intermediate contact pads that allow independent, precise null measurement tests to ensure that all devices are quantized and free of contact resistance errors. These designs allow trimming of the resistance value to classical decade values, such as 10 kΩ or 1000 Ω, with a high level of confidence in the metrological uncertainty.

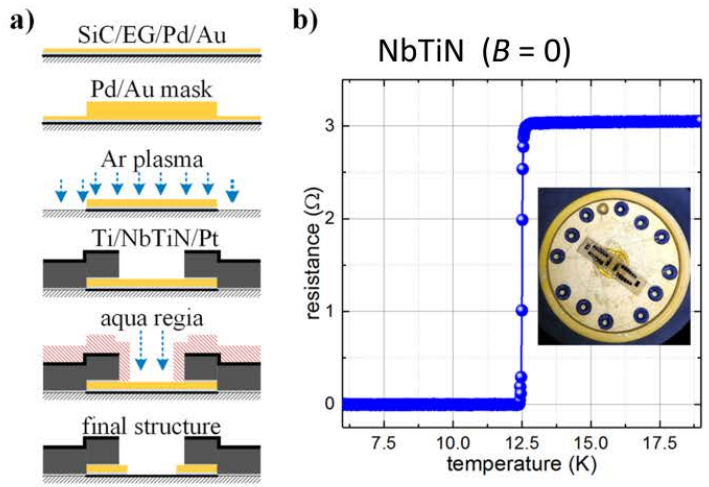

Above, (a) The photolithography process for graphene device fabrication using superconducting NbTiN contacts is divided into six steps (from the top to the bottom) (b) Resistance measurements at $B = 0$ of the superconducting NbTiN material show vanishing resistance below the critical transition temperature $T_c \approx 12.5$ K. The inset represents the top-view onto the sample with two devices mounted on a TO-8 header.

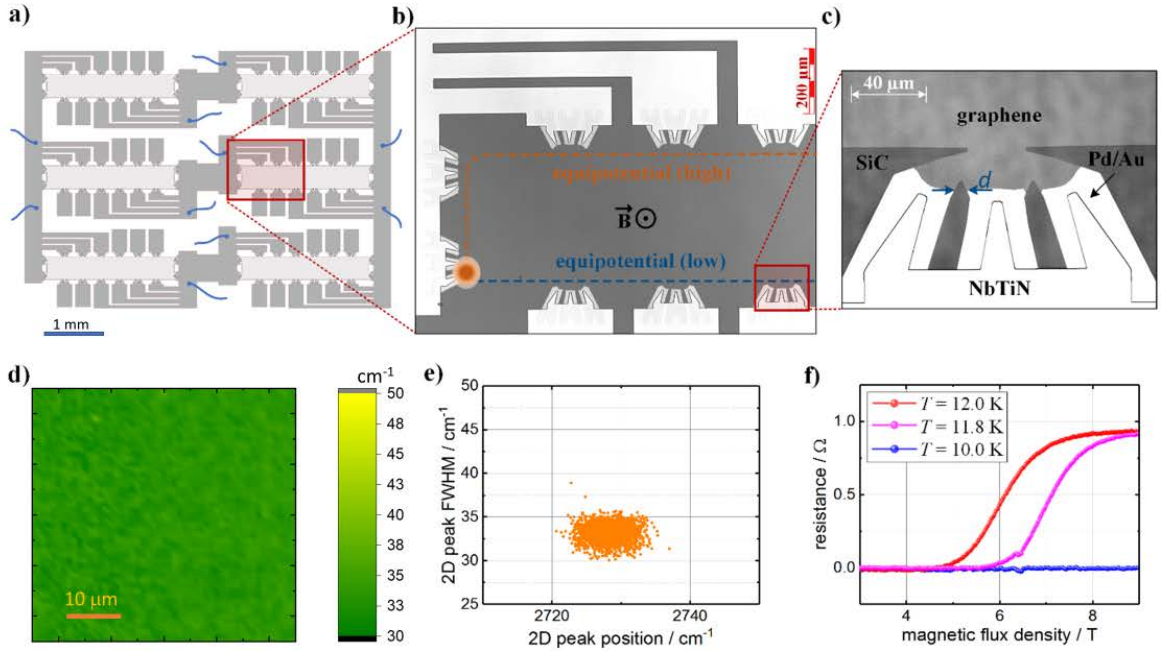

(a) Quantum Hall array design with NbTiN interconnections. (b) Enlarged region of a device shows equipotential at edges and hotspot for one field direction. (c) Split contacts greatly improve contact resistance in the QHE regime[1]. (d) 50 µm × 50 µm area map of 2D band FWHM from Raman spectroscopy. (e) Scatter plot of 2D band FWHM vs. peak position. (f) Graph showing upper critical field transition in a superconducting element of the device.

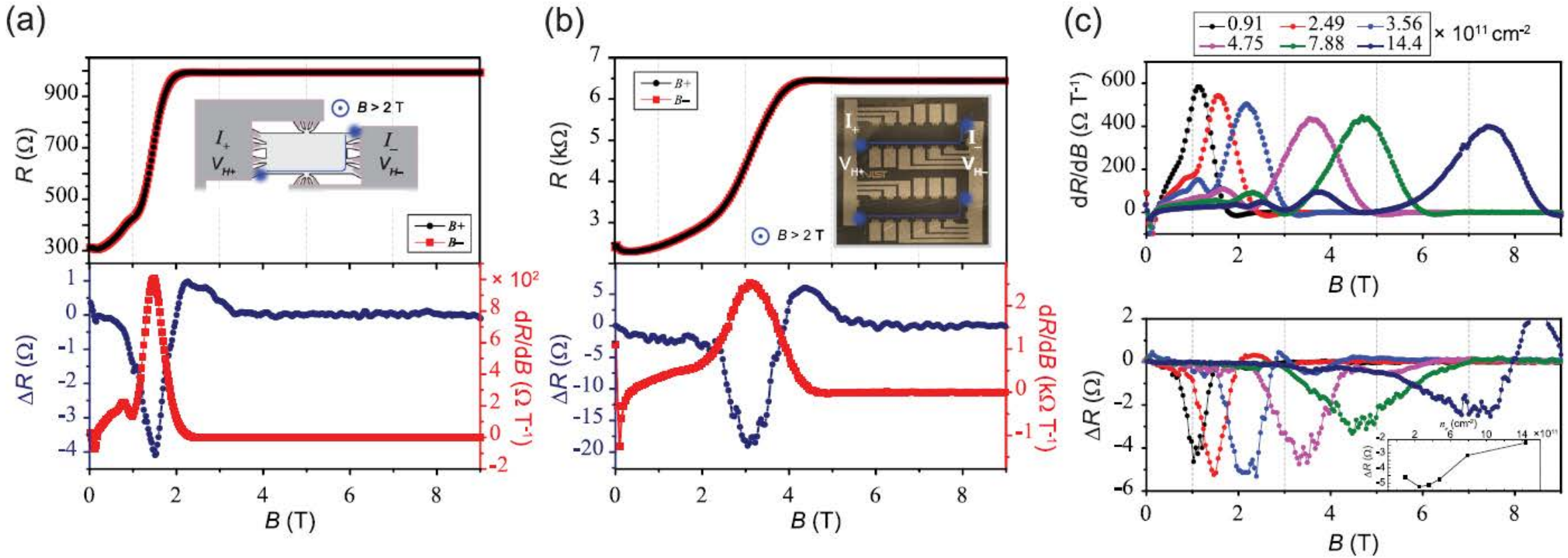

FIG. 4. Measurements using a two-terminal (2-T) device in a four-terminal (4-T) measurement configuration for the (a) 992.8 Ω array and (b) 6.45 kΩ array devices (insets show example equipotential line in solid blue). The top panels show the combined Hall and longitudinal resistance, as well as the corresponding positive B-field measurement configuration, and the bottom panels show ΔR in blue and first derivative of the positive B-field case in red. (c) Both the derivative of the combined resistance curve for the 992.8 Ω array (positive B-field case) and ΔR between the two conditions are shown as a function of electron density. In the ideal case, the bottom panel should yield no differences for devices obeying the Onsager-Casimir relation (OCR).